4-2015

Characterization of Boron Hydride Compounds for Potential Use in Pressurized Water Nuclear Reactors

Alex Blake
Pittsburg State University

CHARACTERIZATION OF BORON HYDRIDE COMPOUNDS FOR POTENTIAL USE IN PRESSURIZED WATER NUCLEAR REACTORS

A Thesis Submitted to the Graduate School
in Partial Fulfillment of the Requirements
for the Degree of
Master of Science

Alex Blake

Pittsburg State University

Pittsburg, Kansas

April, 2015

CHARACTERIZATION OF BORON HYDRIDE COMPOUNDS FOR POTENTIAL USE IN PRESSURIZED WATER NUCLEAR REACTORS

Alex Blake

APPROVED:

Thesis Advisor _____
Dr. Charles Neef, Assistant Professor of Chemistry

Committee Member _____
Dr. William M. Shirley, Professor of Chemistry

Committee Member _____
Dr. James McAfee, Professor of Chemistry

Committee Member _____
Dr. Rebecca Butler, Associate Professor of Physics

CHARACTERIZATION OF BORON HYDRIDE COMPOUNDS FOR POTENTIAL USE IN PRESSURIZED WATER NUCLEAR REACTORS

AKNOWLEDGEMENTS

Special appreciation is expressed to Dr. Charles (Jody) Neef for his continued guidance and allowed use of his laboratory. Gratitude is also expressed to Dr. Ram Gupta for his assistance and expertise in corrosion testing and to Dr William Shirley for his support in NMR testing. A large amount of appreciated assistance was given by Dr. Kevin Cook at 3M's Boron Products plant in Quapaw, Oklahoma.

CHARACTERIZATION OF BORON HYDRIDE COMPOUNDS FOR POTENTIAL USE IN PRESSURIZED WATER NUCLEAR REACTORS

An Abstract of the Thesis by
Alex Blake

The isotope ^{10}B is a good neutron absorber with a thermal neutron absorption cross section of ~3800 barns. This quality has led to the use of boron as a neutron absorber in the nuclear power industry. In current practice, boric acid is commonly used as a neutron absorber in the water regime of active and passive safety systems. The boron hydride compounds in this study, namely $Li_2B_{10}H_{10}$, $Na_2B_{10}H_{10}$, $K_2B_{10}H_{10}$, $Li_2B_{12}H_{12}$, $Na_2B_{12}H_{12}$, and $K_2B_{12}H_{12}$, have been studied to assess their performance in situations where criticality control needs exceed normal control methods. In this type of situation these compounds have several advantages over commonly used neutron absorbers such as boric acid. The boron content of the previously listed boron hydride salts is up to 80 wt% boron compared to 17 wt% for boric acid. The solubility of these compounds is more than ten times greater than boric acid at 25°C. The pH of these compounds has been shown to be neutral in concentrated aqueous solutions. Thermal stability of these compounds as solids has been observed at temperatures greater than 500°C. Electrochemical impedance spectroscopy studies indicated that these compounds are significantly less corrosive than boric acid. Use of these boron hydride salts can lead to reduction in emergency shutdown pool size, reduce or remove the necessity for pool heating and heat tracing of lines, allow for more rapid introduction of the absorber in emergency situations or be used in other applications where significant neutron control is necessary.

TABLE OF CONTENTS

LIST OF TABLES

LIST OF FIGURES

CHAPTER I

INTRODUCTION

Nuclear Industry Background

In November of 2014, 30 countries worldwide were operating 435 nuclear reactors for electricity generation and 72 new nuclear plants are under construction in 15 countries. (*1*) Of these 435 reactors, 224 of them are pressurized water reactors (PWRs). In PWRs neutron poisons or neutron absorbing materials are commonly used to control the rate of fission that is occurring inside the reactor pressure vessel (RPV). A common neutron poison used is boron in the form of boric acid. Of the two naturally occurring isotopes of boron (^{11}B 80%, ^{10}B 20%), ^{10}B is a good neutron absorber with a thermal neutron absorption cross section of ~3800 barns. (*2*) The ability to absorb thermal neutrons while producing benign reaction products makes boron an ideal atom to aid in the control and arrest of the fission reaction in nuclear power reactors. Boric acid, both natural and isotopically enriched, is recommended by the International Atomic Energy Association (IAEA) to be a part of the water chemistry regime in active and passive safety systems. (*3*) Boric acids' use in this type of application has known detriments that

must be strategically mitigated. An example of the problems that can arise from boric acids' use was found in early March 2002 at the Davis-Besse nuclear power station in Oak Harbor Ohio. (*4*) At this plant, it was discovered during an inspection that between 650 and 980 cubic centimeters of metal had corroded and been flushed away from the RPV head, leaving only a thin layer of steel cladding about 7.6 mm (0.3 in.) thick. This incident shows that boric acid, while it is a weak acid with a pH of 3-4 for concentrated solutions, can cause significant damage to power plant construction materials under elevated pressure and temperatures.

Boric Acids Use in Emergency Situations

Boric acid is commonly used in emergency situations as well. In November of 2011 the Tokyo Electric Power Company (TEPCO) detected the possible presence of radioactive gases from inside the primary containment vessel (PCV) of unit 2 from the tsunami damaged Fukushima Daiichi Nuclear power station in Japan. (*5*) In response to this detection 10 tons of boric acid solution (water containing 480 kg of boric acid) was injected into the PCV. This amount of material had to be injected in less than one hour. In this and other emergency situations a need exists for a thermal neutron absorber that possesses superior technical advantages to boric acid.

Project Rationale

Neutron absorber advantages should include a material that is less damaging to commonly used nuclear containment materials like steel and be more soluble than boric

acid thus decreasing the total volume of water needed and reducing the possibility of leaks or safety line systems rupturing. As much of the chemistry involved in nuclear safety is heavily regulated a desirable replacement for boric acid would be one that has a similar chemical makeup. Continuing to use boron as the neutron absorber would be preferred as it is readily available, an effective thermal neutron absorber, and widely used. In summation, when taking into consideration the requirements for a superior neutron absorber it is essential that the material have a similar chemical composition, high boron content, high solubility in water, a high thermal stability given the high temperatures that are common practice in the nuclear energy industry, and be less corrosive.

In the nuclear industry boric acid has caused problems by corroding power plant construction materials as mentioned previously at the Davis-Besse nuclear power station in Oak Harbor Ohio. With this specific instance in mind a need arises for the chosen boron compound in this study to be less corrosive. Determining whether or not a boron compound will be corrosive can be difficult. The data from the Davis-Besse nuclear power station shows that boric acid, under the right conditions, is extremely corrosive. (*4*) However, a review of a patent by Bommaraju shows that the corrosion rate of stainless steel immersed in an aqueous solution of alkali metal hydroxide could be inhibited by adding 2 to 300 ppm of sodium borohydride. (*6*) These data show a different perspective than what was observed at the Davis-Besse nuclear power station. Another study by Suwattananont and Petrova at the New Jersey Institute of Technology used Tafel plots to show that steel coated with a boronizing powder mixture consisting of B_4C and KBF_4 improved the steel's microhardness and corrosion resistance. (*7*) It is beneficial to see

that sodium borohydride inhibits corrosion and improves microharndess as demonstrated by electrochemical Tafel data, what remains to be seen however is if a boron hydride compound will be less corrosive to a steel substrate than boric acid. This presents another area of focus to understand the use of boron hydrides as neutron absorbers.

Boron Hydrides

Boron hydrides were first discovered by Alfred Stock in 1912. (*8*) An industrial use for these compounds did not exist until after World War II when pentaborane, B_5H_9, and decaborane, $B_{10}H_{14}$, were believed to be extremely powerful fuels for use in aeronautic engineering. (*9*) This boom in boron hydride chemistry was fueled by the US and Russian militaries investing millions of dollars and rubles into the use of these materials as rocket fuels. While the idea of these compounds being used as a propellant was eventually abandoned the foundation of a new field of study was laid for boron hydride and borane research. The first significant understanding of boron hydride chemistry came in 1963 from William N. Lipscomb and his proposal of a three-center two-electron bond. (*10*) This was followed by further classification of the main types of deltahedra by Robert E. Williams in 1971. (*11*) Moving on from these initial discoveries a rich field of boron hydride chemistry has been developed, fueled by boron's ability to form self-bonded complex networks as vast as any natural element save carbon.

From this field of study the literature shows promising data for the use of boron hydrides as neutron absorbers. Muetterties found that the salts of both the $B_{10}H_{10}^{-2}$ and

the $B_{12}H_{12}^{-2}$ anions are thermally stable, up to 810° C for Cesium salts. (*12*) These data show that the thermal stability of these anions is truly surprising. Corroborating thermodynamic data from Kaczmarzyk showed that compared to most boranes, the polyhedral ions of $B_{10}H_{10}^{-2}$ and $B_{12}H_{12}^{-2}$ exhibit unusual thermal stability as evident by their standard enthalpies of formation, 92.1 kJ per mole for $B_{10}H_{10}^{-2}$ and 46.1 kcal per mole for $B_{12}H_{12}^{-2}$. (*13*) Also of interest are the data from Muetterties which points out that $Na_2B_{10}H_{10}$ and $Na_2B_{12}H_{12}$ have an oral toxicity to rats that is comparable to sodium chloride, which is important given the environmental restrictions in the nuclear industry. (*12*) The solubility of these compounds, as mentioned before, is of interest to hopefully increase the ease of use and the overall safety of the chemical system. It is encouraging to see that the literature shows that small unipositve cations combined with the $B_{10}H_{10}^{-2}$ and the $B_{12}H_{12}^{-2}$ anions form water-soluble salts isolated as hydrates. (*12*) Promising data are also available showing sodium pentaborate's (NaB_5O_8) solubility to be 12.20 grams per 100 grams of saturated solution at 25°C. (*14*) This value is more than double that of boric acid with a value of 4.72 grams per 100 grams of saturated solution at 25°C. When presented with the thermal stability, low toxicity, and high solubility of alkali salts of the $B_{10}H_{10}^{-2}$ and the $B_{12}H_{12}^{-2}$ anions these materials were chosen as the focus of this study.

Structure of the $[B_{10}H_{10}]^{2-}$ and $[B_{12}H_{12}]^{2-}$ anions

The structures of both the $[B_{10}H_{10}]^{2-}$ and $[B_{12}H_{12}]^{2-}$ anions are known. (*15*) (*16*) The $[B_{10}H_{10}]^{2-}$ anion in Figure 1 has a bi-pyramidal formation while the $[B_{12}H_{12}]^{2-}$ anion in Figure 2 is icosahedral.

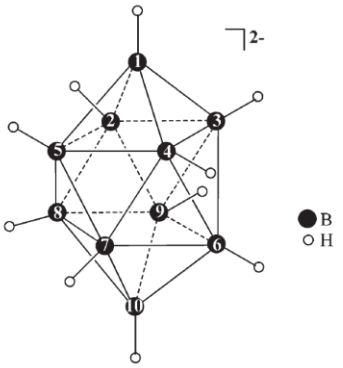

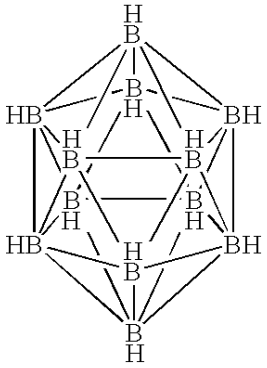

Figure 1: Structure of $[B_{10}H_{10}]^{2-}$ anion (*15*) **Figure 2: Structure of $[B_{12}H_{12}]^{2-}$ anion (*16*)**

These structures demonstrate the ability of boron to form a complex self-bonded network. Having a broader understanding of polyhedral boron structures yields an increased desire for their application as neutron absorbers in the nuclear industry simply due to the level of boron observed in these structures. Compared to boric acid with a chemical formula of $B(OH)_3$, boric acid has one boron per mole of boric acid and is 17.49% by weight assuming natural abundance isotopic distribution. In fact due to their high boron content and thermal neutron absorption capabilities, complex boron hydride compounds similar to those shown above have been frequently studied in the field of neutron capture therapy. Indeed, applicable information within the neutron capture field is available that directly parallels much of the data presented in this research

Useful Information from Neutron Capture Therapy

Research involving neutron capture therapy can be found as early as 1936 by Locher, with boron being incorporated as the neutron absorber in 1940 by Kruger. (*17*) (*18*) Neutron capture therapy is a procedure for achieving selective irradiation of

diseased cancerous tissue by inducing radioactivity throughout that tissue. The radioactivity is induced *in situ* by the capture of thermal neutrons by a stable target element. The early data from this field supports the use of boron as a neutron absorber with corroborating data on its thermal neutron absorption cross section and its toxicology. (*19*) As the desire to develop a method that selectively destroys malignant cells in the presence of normal cells is a highly valued goal, much effort has been given to the study of different boron complexes to achieve this goal. From these efforts it has been observed how a B_{10} cage could be fused to a B_{12} cage. (*20*) Also of interest is a study by Avdeeva published in 2014 which describes reactions with triethylammonium closo-decaborate, $(Et_3NH)_2B_{10}H_{10}$, to isolate different cationic compounds which were synthesized by quantitative precipitation from aqueous solution by the exchange reaction of $(Et_3NH)_2B_{10}H_{10}$. (*21*) The two aforementioned studies provide useful information furthering the understanding of the functionality of the $B_{10}H_{10}^{2-}$ anion and how it can be coupled with a wide array of cations.

After studying the literature and gaining a better understanding of the requirements of thermal neutron absorbing materials, the compounds chosen for this study are lithium, sodium and potassium salts of the $B_{10}H_{10}^{2-}$ and $B_{12}H_{12}^{2-}$ anions. It is Muetterties who points out that water-soluble salts of $B_{10}H_{10}^{2-}$ and $B_{12}H_{12}^{2-}$ are most conveniently prepared from their corresponding aqueous free acids by exact neutralization. (*12*) What is now needed is a chemical characterization of these compounds including their initial synthesis, hydration levels, solubility, pH and stainless steel corrosion rate measured by electrochemical impedance.

CHAPTER II

EXPERIMENTAL

Starting Materials

Triethylammonium decaborate, $(Et_3NH)_2B_{10}H_{10}$, and triethylammonium dodecaborate, $(Et_3NH)_2B_{12}H_{12}$ were received from Boron Specialties in Ambridge Pennsylvania via Beth Bosley. Amberlite IR -120 resin was purchased from Alfa Aesar, for cation exchange. Resin was placed inside two Ace epoxy coated, 76 mm diameter, and 635 mm length, glass columns with a coarse fitted filtering disk and 2 mm bore Teflon stopcock. Columns were acidified using 1.5M hydrochloric acid (HCl(aq)) prepared from concentrated HCl purchased from Sigma Aldrich (SA). Lithium hydroxide (>98.0%), sodium hydroxide (>97.0%) and potassium hydroxide (>85.0%) were used, all purchased from SA. Toluene, used with a Dean-Stark trap, was also purchased from SA. Natural boric acid, also purchased from SA, was used as a benchmark in pH, solubility, and corrosion testing. For pH testing three standards with pHs of 4.01, 7.00, and 10.01 were received from Orion Application Solutions purchased from Thermo Scientific and were certified traceable to NIST standard reference material.

For use in electrochemical impedance testing as working electrodes type 304 stainless steel coupons were purchased from Rohrback Cosasco Systems.

Characterization

NMR, Boron Content, and pH

Proton nuclear magnetic resonance (^{1}H NMR) and boron nuclear magnetic resonance (^{11}B NMR) spectra were collected using a Bruker UltraShield 500MHz NMR with D_2O as the solvent. Boron trifluoride diethyl ehterate was used as the zero reference in the ^{11}B NMR. The spectra collected from the NMR testing were useful in assessing each B_{10} and B_{12} boron hydride's chemical makeup and purity. As boron is the only source of neutron absorption in boric acid for the context of this study, data was collected on a boron content basis. Thermogravimetric analyses were performed on a TA instrument TGA Q500, using 8 to 10 milligrams of compound. Samples were heated under nitrogen using a heating ramp of 10^{o}C/min from room temperature to 590^{o}C. The pH of each boron hydride salt was measured using a Fisher pH/Ion 510 pH meter which was calibrated in accordance with the Fisher Science Education pH/Ion 510 manual. The amount of each compound used was boron weight equivalent to a concentrated boric acid solution at room temperature. All materials were dissolved in degassed deionized water. The pH of each solution was measured before the compound was added, upon compound addition, after stirring for 5 minutes, 10 minutes, and 15 minutes.

Solubility

The solubilities of each borohydride salt were measured by following the Organisation for Economic Co-operation and Development (OECD) procedure. (*22*) This was done by placing 3 grams of each compound (+/- 0.1 gram) in an appropriately sized graduated cylinder, adding small aliquots of water (0.1mL to 1mL to 2mL) from a calibrated pipette, stirring for ten minutes, observing if the material was in solution and adding more water if necessary until all the material was in solution. This test was performed for each compound at four different temperatures 4 °C, 22 °C, 40 °C and 60 °C. For the tests at 40, and 60°C the graduated cylinder was partially immersed into a water bath set at the desired temperature. For the 4 °C test the bath was filled with silicon oil instead of water. The same test was also performed on boric acid as a test control.

Electrochemical Impedance Spectrum (EIS)

EIS was measured using a Princeton Applied Reasearch VersaSTAT 4 potentiostat/galvanostat equipped with a 15 cm long platinum counter electrode and a silver chloride single junction 14/20 adapter reference electrode both from Pine Research Instrumentation. The stainless steel coupons were used as the working electrodes. A concentrated boric acid solution was made by dissolving 10.848 grams of boric acid in 225 mL of water at 22 °C. This equates to 1.897 g of boron. The amount of each boron hydride compound used was boron weight equivalent to the concentrated boric acid solution at 22 °C. Using digital calipers an area of 2.55 x 1.25 x 0.15 cm of the steel coupon was measured and submerged in 150 mL of each compounds solution. The

corrosion rate (Icorr) was evaluated using a Tafel plot which plotted the Current (A) versus Potential (V). (*23*) The Tafel plot was carried out by using an initial potential of -0.25V and final potential of 0.25V. The scan properties were a step height of 5mV, a step time of 1 second and 101 total points collected. This test was performed at both 22 °C and 80 °C.

Synthesis

$Li_2B_{10}H_{10}$ Synthesis

$Li_2B_{10}H_{10}$ salt synthesis was performed by using 1500 grams of Amberlite IR - 120 resin. This column was rinsed several times with deionized (DI) water to remove impurities and then acidified with 2 L of 1.5M HCl. The acid was allowed to flow through the column at a rate of approximately 7 mL per minute. Once the 2 liters of HCl passed through the column, the column was again rinsed with DI water to neutrality. $(Et_3NH)_2B_{10}H_{10}$ [200.24 g (0.61 mols)] in DI water (3.5 L) was then loaded onto the acidified column. This material was allowed to undergo cation exchange by flowing through the column at a rate of approximately 5 mL per minute. The expected eluent from the column was the acid $H_2B_{10}H_{10}$. It was evident that this was the aqueous solution obtained as the pH of the column eluent, as measured by pH paper, changed from neutral to strongly acidic. This pH change was useful in indicating when the acid elution started and ended. In each case additional deionized water was required to fully rinse all of the protonated borohydride acid off of the column. Once all of the acid was collected, roto-evaporation was used to condense the volume to 1 L of $(H_3O)_2B_{10}H_{10}$. The calculated

molarity of this solution was 0.61. Next, using 300 mL of this acid, a titration with 2M lithium hydroxide solution (LiOH) was carried out to neutrality, with the final product being $Li_2B_{10}H_{10}$. To remove most of the water a Dean Stark trap was used with a toluene azeotrope. Percent yield for the $Li_2B_{10}H_{10}$ was 108%. Proton and boron NMR for $Li_2B_{10}H_{10}$ are shown in APPENDIX B. ^{1}H NMR (D_2O): δ (ppm) 3.8-2.9 (m, 2H), 0.5- ˉ 0.5 (m, 8H). ^{11}B NMR (D_2O) -1 (d, 2B) -30 (d, 8B).

$Na_2B_{10}H_{10}$ Synthesis

Synthesis for the $Na_2B_{10}H_{10}$ followed the same process as the $Li_2B_{10}H_{10}$ synthesis, except when titrating, sodium hydroxide (NaOH) was used instead of LiOH. Percent yield for the $Na_2B_{10}H_{10}$ was 104%. Proton and boron NMR for $Na_2B_{10}H_{10}$ are shown in APPENDIX B. ^{1}H NMR (D_2O): δ (ppm) 3.8-2.9 (m, 2H), 0.5- ˉ0.5 (m, 8H). ^{11}B NMR (D_2O) -1 (d, 2B) -30 (d, 8B).

$K_2B_{10}H_{10}$ Synthesis

Synthesis for the $K_2B_{10}H_{10}$ followed the same process as the $Li_2B_{10}H_{10}$ synthesis, except when titrating, potassium hydroxide (KOH) was used instead of LiOH. Percent yield for the $K_2B_{10}H_{10}$ was 101%. Proton and boron NMR for $K_2B_{10}H_{10}$ are shown in APPENDIX B. ^{1}H NMR (D_2O): δ (ppm) 3.8-2.9 (m, 2H), 0.5- ˉ0.5 (m, 8H). ^{11}B NMR (D_2O) -1 (d, 2B) -30 (d, 8B).

$Li_2B_{12}H_{12}$ Synthesis

In order to load the B_{12} ammonium salt onto the column the $(Et_3NH)_2B_{12}H_{12}$ was first combined with potassium hydroxide until a pH of > 9 was reached. This was done

because the $K_2B_{12}H_{12}$ salt is more soluble than the ammonium salt. To help eliminate contamination this cation exchange used different Amberlite IR-120 resin than was used for the B_{10} salts. The amount of resin and triethylammonium boron salt used was the same as the B_{10} synthesis. Once the $H_2B_{12}H_{12}$ acid was isolated, just as with the B_{10} acid, a titration was performed with lithium hydroxide yielding the desired salt $Li_2B_{12}H_{12}$ salt. Finally, to remove water and isolate the compound, after titration a Dean Stark trap with a toluene azeotrope was used. Percent yield for the $Li_2B_{12}H_{12}$ was 106%. Proton and boron NMR for $Li_2B_{12}H_{12}$ are shown in APPENDIX B. ^{1}H NMR (D_2O): δ(ppm) 0.5- ¯0.5 (m, 12H). ^{11}B NMR (D_2O) -15 (d, 12B).

$Na_2B_{12}H_{12}$ Synthesis

Synthesis for the $Na_2B_{12}H_{12}$ followed the same process as the $Li_2B_{12}H_{12}$ synthesis, except when titrating sodium hydroxide (NaOH) was used instead of LiOH. Percent yield for the $Na_2B_{12}H_{12}$ was 105%. Proton and boron NMR for $Na_2B_{10}H_{10}$ are shown in APPENDIX B. ^{1}H NMR (D_2O): δ (ppm) 0.5- ¯0.5 (m, 12H). ^{11}B NMR (D_2O) -15 (d, 12B).

$K_2B_{12}H_{12}$ Synthesis

Synthesis for the $K_2B_{12}H_{12}$ followed the same process as the $Li_2B_{12}H_{12}$ synthesis, except when titrating, potassium hydroxide (KOH) was used instead of LiOH. Percent yield for the $K_2B_{10}H_{10}$ was 100%. Proton and boron NMR for $K_2B_{10}H_{10}$ are shown in APPENDIX B. ^{1}H NMR (D_2O): δ (ppm) 0.5- ¯0.5 (m, 12H). ^{11}B NMR (D_2O) -15 (d, 12B).

CHAPTER III

RESULTS AND DISCUSSION

Synthesis (Results)

The ^{1}H NMR spectrum of $((CH_3CH_2)_3NH)_2B_{10}H_{10}$ is shown in Figure 3. This is the spectrum of the starting material before cation exchange was performed. The two largest peaks at 1.1ppm and 3ppm are attributed to the protons on the three ethyl groups. The peak at 4.6ppm is due to water. The two multiplets centered at 3.2ppm and 0ppm are attributed to the protons on the boron cage and can be seen better in the spectrum of $Li_2B_{10}H_{10}$ shown in **Error! Reference source not found.**. The cage structure of the $_{10}H_{10}^{2-}$ anion, as shown previously in Figure 1, possesses two different proton signals from the boron cage. The protons in the axial position are one (3.2 ppm) and the protons in the equatorial being the other (0ppm). Boron has two known spins with the ^{10}B isotope having a spin, 'I', value of 3 and the ^{11}B isotope a value of 3/2.

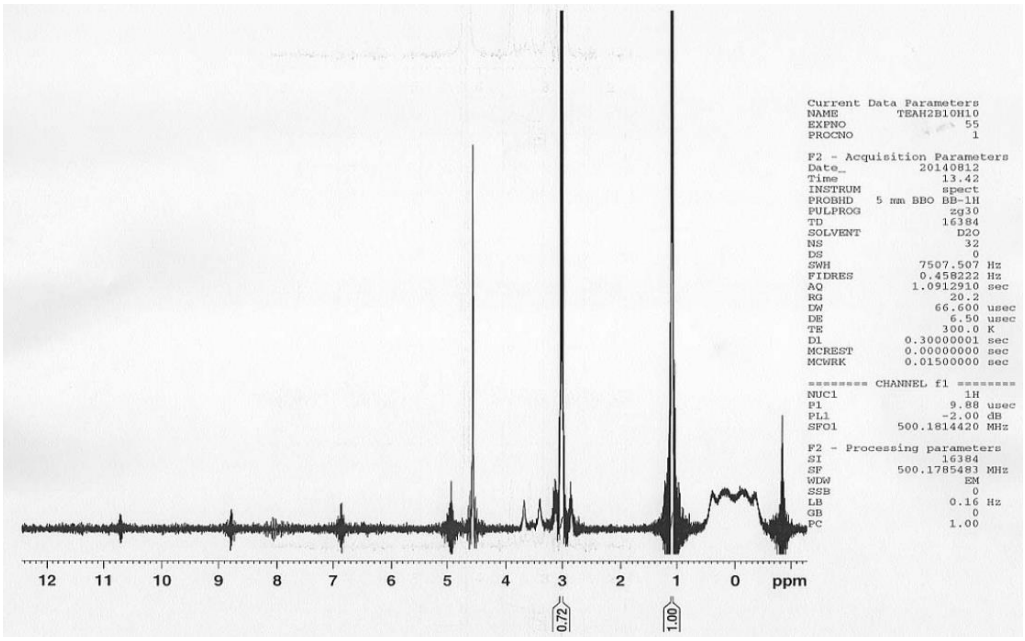

Figure 3: ^{1}H NMR of $((CH_3CH_2)_3NH_2)B_{10}H_{10}$

Using the equation 2I+1 it can be expected that the boron proton signal would be a septet for ^{10}B and quartet for ^{11}B. In **Error! Reference source not found.** this splitting can be een in the multiplet centered at 3.2ppm. The four larger peaks show the ^{11}B quartet and three peaks of the ^{10}B septet can be seen with the remaining four being covered by the ^{11}B quartet. This interpretation of the spectra matches previous literature. (10) It can also be observed, from the spectra in Figure 3 and **Error! Reference source not found.**, hat the large tri-ethyl peaks have been greatly reduced, which was consistent with ion exchange.

The spectra show evidence of the loss of the tri-ethyl groups but with small amounts still remaining. This reduction of the amount of tri-ethyl in each compound can be seen in all the boron hydride salts' spectra. One major difference between the B_{10} and B_{12} boron hydride proton spectrums is the lack of the multiplet centered at 3.2 ppm in the

B_{12} ^{1}H NMR spectrum, as seen in Figure 5. This is due to the symmetry of the $B_{12}H_{12}$ boron cage as an icosahedron.

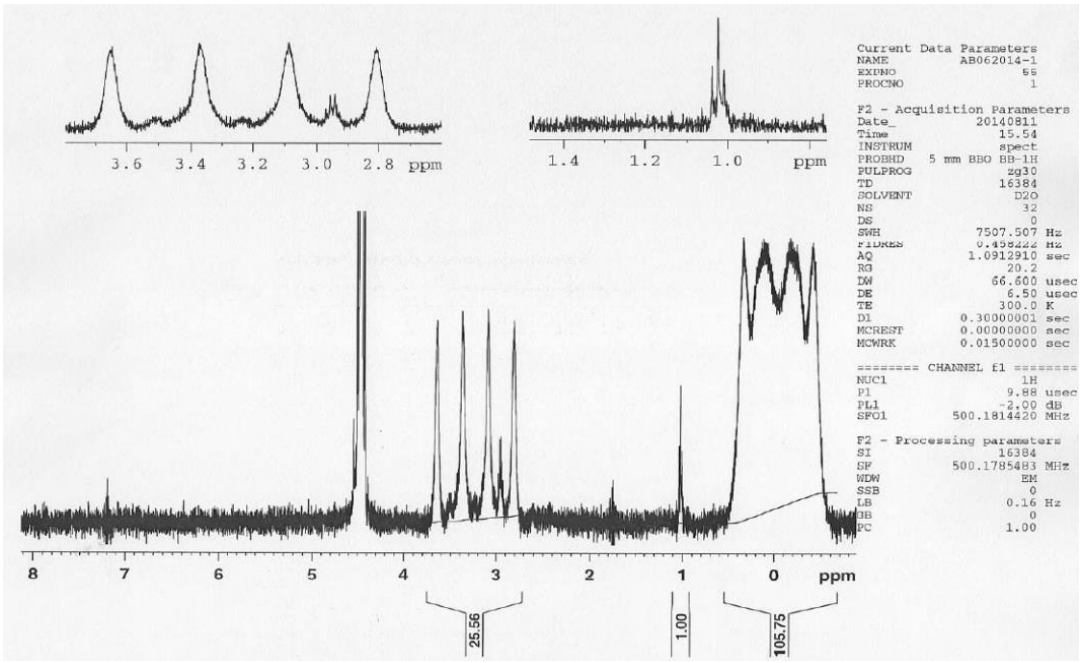

Figure 4: ^{1}H NMR of $Li_2B_{10}H_{10}$

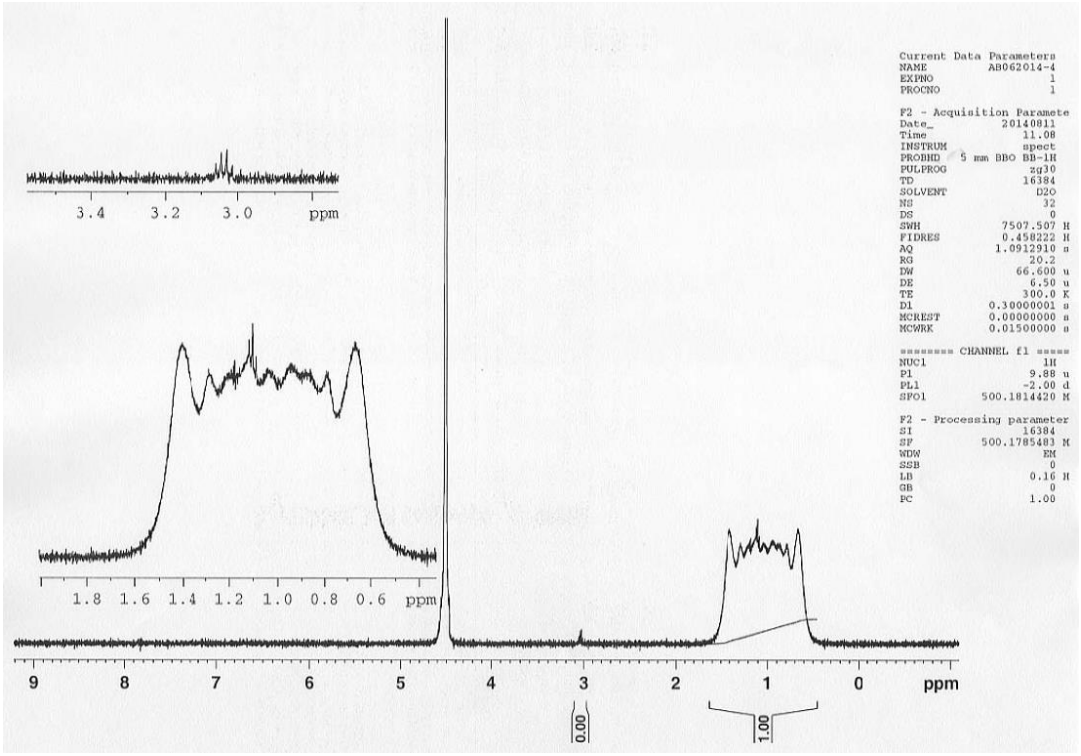

Figure 5: ^{1}H NMR of $Li_2B_{12}H_{12}$

^{11}B NMR was also collected and can be seen in Figure 6 for $K_2B_{10}H_{10}$ and in Figure 7 for $K_2B_{12}H_{12}$. The doublets observed are due to the coupling of the ^{1}H-^{11}B within the boron cage.

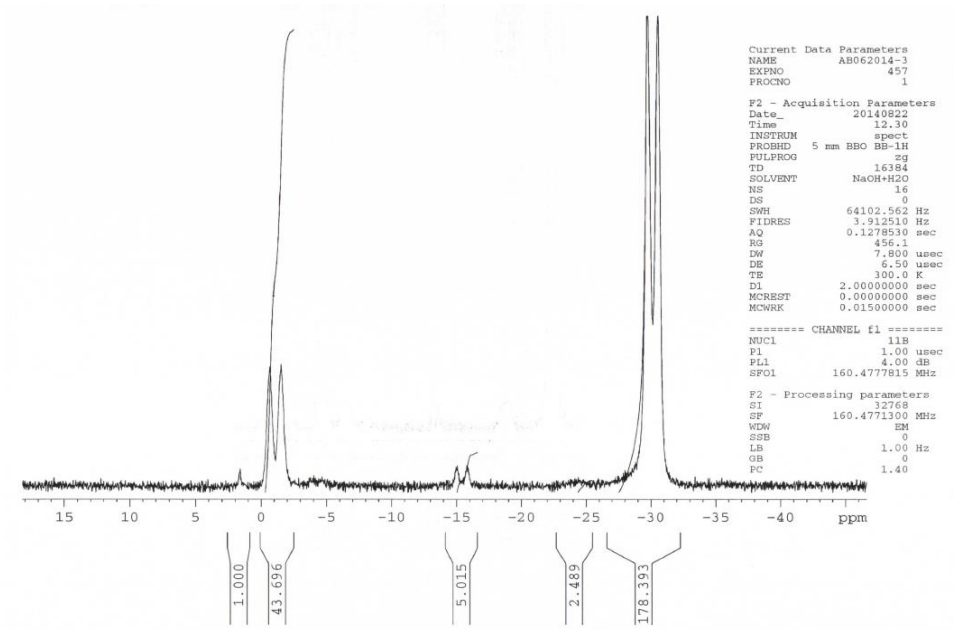

Figure 6: ^{11}B NMR of $K_2B_{10}H_{10}$

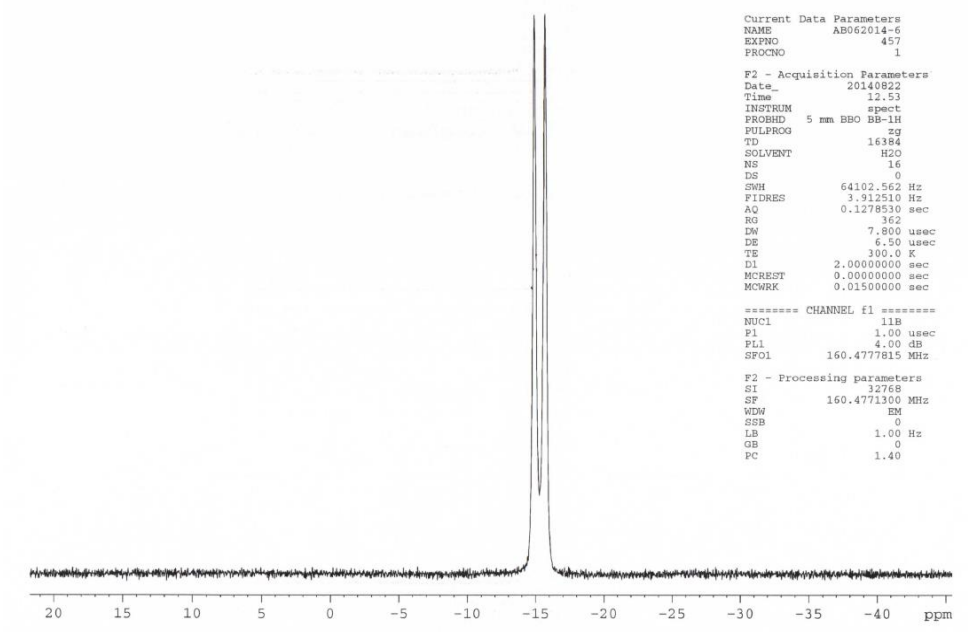

Figure 7: ^{11}B NMR of $K_2B_{12}H_{12}$

From these ^{11}B NMR spectra the difference in the symmetry of the two boron cages can again be seen. Figure 6 shows the two boron cage signals at -1 for the axial and -30 for the equatorial. The small peak at -15 shows a residual amount of B_{12} that was present in

the starting material as an impurity from the synthesis of the triethylammonium decaborate. Thus, in Figure 7 the only observable peak is the single boron signal from the icosahedral boron cage. This same boron spectrum was seen for all of the compounds. All of the NMR spectrum can be found collectively in APPENDIX B.

Boron Content

The TGA data for $Li_2B_{10}H_{10}$, $Na_2B_{10}H_{10}$, and $K_2B_{10}H_{10}$ are shown in Figure 8.

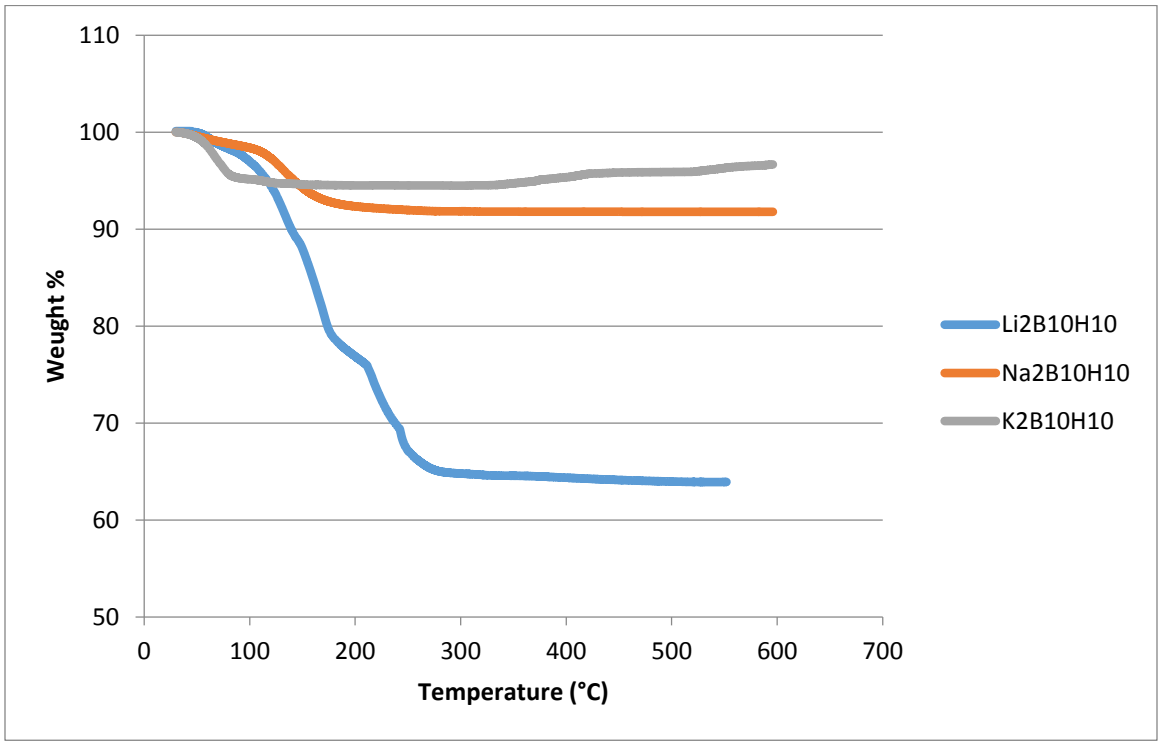

Figure 8: TGA data of $Li_2B_{10}H_{10}$, $Na_2B_{10}H_{10}$ and $K_2B_{10}H_{10}$

With a chemical formula of $B(OH)_3$, boric acid has one boron per mole of boric acid and is 17.49% by weight assuming natural abundance isotopic distribution. With formulas of $B_{10}H_{10}^{2-}$ and $B_{12}H_{12}^{2-}$ these boron hydride anions have ten to twelve times more boron

than boric acid. Since boron is the only neutron absorber in boric acid this provides a significant advantage in the nuclear safety industry. Each of these compounds experienced a weight loss starting at approximately 100°C. This is due to water that is contained in each compound's crystal structure as a hydrate. The lithium compound was by far the most hydrated as a total weight loss of 36.03% was observed. Similar data were also recorded for the B_{12} salts. Table 1 shows the TGA data for all boronhydride compounds.

Table 1: TGA data of Boron Hydride compounds

Compound	Total Weight % Lost	Weight % lost in temperature ranges				
		30-100°C	100-200°C	200-300 °C	300-400 °C	400-500 °C
$Li_2B_{10}H_{10}$	36.03%	3.02%	20.11%	12.08%	0.43%	0.39%
$Na_2B_{10}H_{10}$	8.21%	1.62%	6.04%	0.51%	0.04%	0.00%
$K_2B_{10}H_{10}$	5.52%	4.86%	0.64%	0.02%	0.00%	0.00%
$Li_2B_{12}H_{12}$	34.72%	5.71%	14.52%	14.11%	0.00%	0.38%
$Na_2B_{12}H_{12}$	14.41%	6.54%	6.74%	0.26%	0.77%	0.10%
$K_2B_{12}H_{12}$	10.59%	0.44%	9.19%	0.32%	0.64%	0.00%

This level of hydration is of interest when testing these boronhydride compounds against boric acid on a boron content basis. Once a stable temperature was reached in the TGA testing the percentage of weight lost was assumed to be water. This percentage was then used to calculate the level of hydration. For example the percentage of 36.03 was used to determine the level of hydration for the $Li_2B_{10}H_{10}$. This was done by multiplying the compounds molecular weight (132.07 g/mol) by the value (0.3603) and then dividing by the molecular weight of water (18 g/mol). For the $K_2B_{10}H_{10}$ it was unclear why the compound started to slightly gain weight after 300 °C. For this compound the percentage 5.50 was used in the calculation.

From the TGA data the level of hydration of each salt, as shown by the following formulas, was found to be: $Li_2B_{10}H_{10}$•2.6H_2O, $Na_2B_{10}H_{10}$•0.7H_2O, $K_2B_{10}H_{10}$•0.6H_2O, $Li_2B_{12}H_{12}$•3H_2O, $Na_2B_{12}H_{12}$•1.5H_2O and $K_2B_{12}H_{12}$•1.3H_2O. This data shows that these boron hydrides are 50-60% boron by weight after taking into consideration the amount of hydration for each compound. As further efforts are made to develop methods to remove the water that is present in each compound the percent of boron could increase to up to 80% boron once the material is anhydrous. This percentage of boron in each compound means an extremely significant increase in the amount of neutron capture that can be achieved compared to boric acid. The data collected from the TGA analysis, Table 1, also showed that these compounds are stable up to 500 °C. This evidence, coupled with the high boron content, is crucial when considering these compounds as neutron absorbers. With pressure water and boiling water reactor core temperatures commonly in the 200 to 500 °C temperature range, it is vital to have a compound that will not degrade at such temperatures.

Solubility

Once the level of hydration of each compound was obtained solubility data was calculated on a boron content basis. Figure 9 shows the solubility of the B_{10} salts while Figure 10 shows the solubility of the B_{12} salts. The full solubility testing data can be found in APPENDIX A. The results of the solubility testing show that each boron hydride compound possesses a significantly higher solubility in water than boric acid at every temperature investigated.

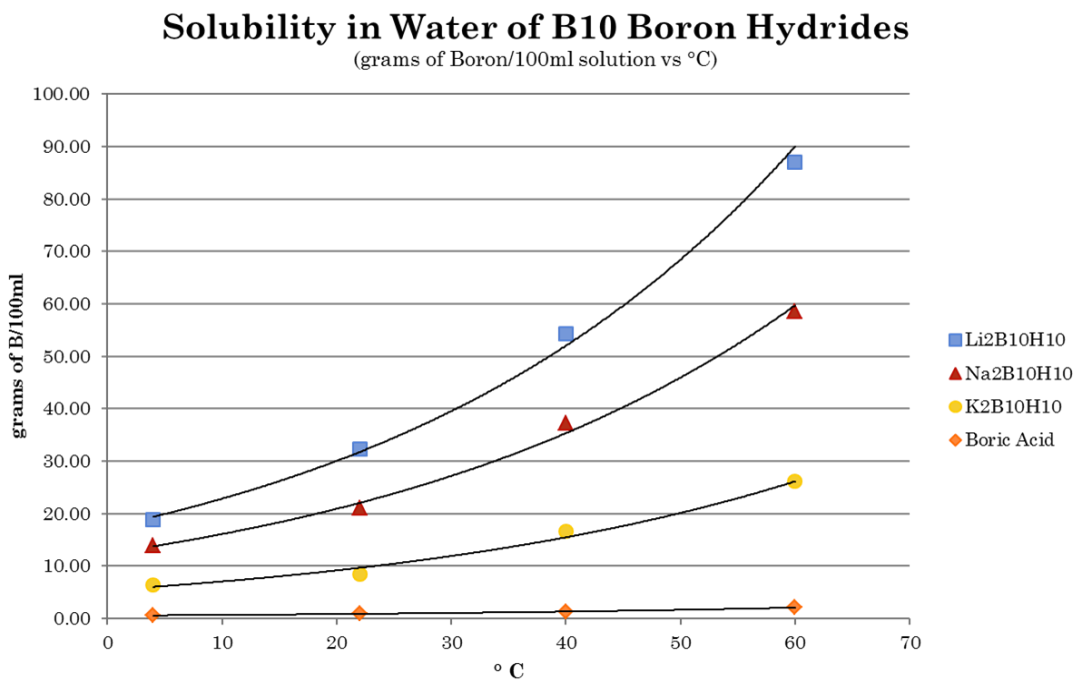

Figure 9: Graph of B_{10} salts solubility data

At 4°C, boric acid has a boron solubility of less than 1 g/100 mL of solution, while $Li_2B_{10}H_{10}$ has over 18 g of soluble boron/100 mL of solution, $Na_2B_{10}H_{10}$ over 13 g and $K_2B_{10}H_{10}$ over 6 g. Similar results are shown for the B_{12} salts in Figure 10. It can be seen that this trend grows exponentially as the temperature is increased. At 60°C boric acid has just over 2 g of soluble boron/100 mL of solution, while $Li_2B_{10}H_{10}$ and $Li_2B_{12}H_{12}$ are over 60 g, $Na_2B_{10}H_{10}$ and $Na_2B_{12}H_{12}$ over 45 g and $K_2B_{10}H_{10}$ and $K_2B_{12}H_{12}$ over 25 g.

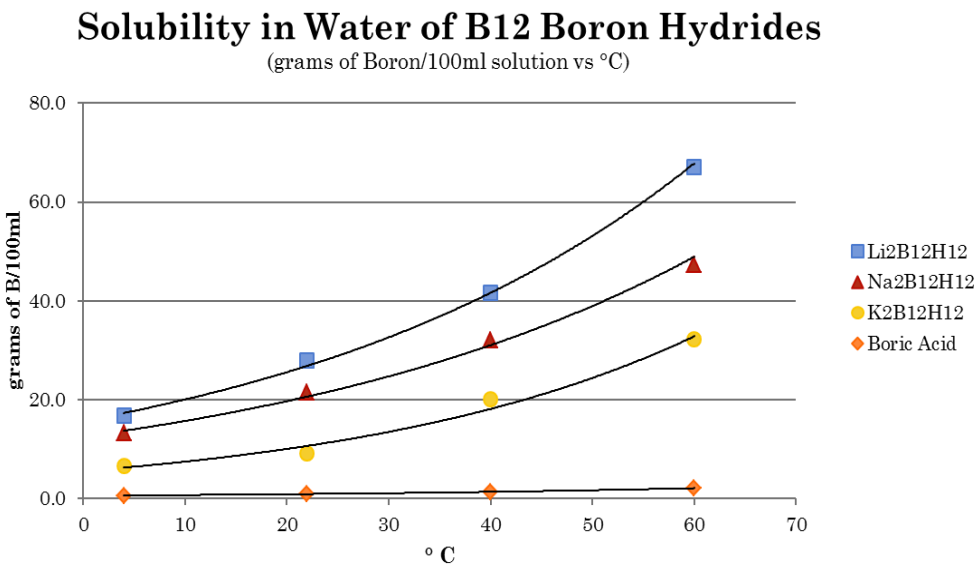

Figure 10: Graph of B_{12} salts solubility data

These data demonstrate the high boron solubility of these compounds. This is a fundamental consideration in emergency shutdown situations. With these levels of boron solubility the volume of water needed is drastically reduced when compared to the levels needed using boric acid as the neutron absorber. Additionally, often in nuclear water safety systems heat traced lines are used to keep the high concentration neutron absorbers (boric acid) in solution. (*24*) With the available solubility of these boron compounds heat tracing would not be necessary, even for concentrated solutions. Nuclear facilities are required to keep accurate measurements and surveillance systems for the reactor water that is in use. (*25*) (*26*) There is a direct correlation between the volume of water used and the difficulty in accurately measuring and controlling the water safety system. When the amount of water required to maintain regulated safety standards is decreased the

difficulties involved in this safety program are also reduced. It was observed that the B_{12} salts were slightly less soluble than the B_{10}, this trend is consistent with literature. (*12*)

pH of Boronhydride Compounds

Table 2 shows the pH comparison of the boron hydride compounds and boric acid.

Table 2: pH Comparison of Boron Hydrides and Boric Acid

Time (min)	Compound pH						
	$Li_2B_{10}H_{10}$	$Na_2B_{10}H_{10}$	$K_2B_{10}H_{10}$	$Li_2B_{12}H_{12}$	$Na_2B_{12}H_{12}$	$K_2B_{12}H_{12}$	Boric Acid
Before addition	6.47	6.48	6.44	6.55	6.48	6.50	6.54
5 minutes	6.77	6.70	6.92	6.68	6.83	6.86	4.20
10 minutes	6.80	6.81	6.98	6.73	6.91	7.03	3.91
15 minutes	6.79	6.81	6.98	6.72	6.90	7.03	3.91

These data show that aqueous solutions of these compounds have a neutral pH change when compared to boric acid. It is a significant advantage in the nuclear industry for these compounds to possess a neutral pH. This indicates that these compounds are less damaging and easier to incorporate into a water chemistry system. The overall pH of these compounds can be seen to be neutral as well. As the synthesis of these compounds involves using a strongly basic hydroxide as the titrant it is assumed that the increase in pH for each compound is a reflection of excess hydroxide present in the compound. This is evidence of the need to further reduce residual hydroxide levels from the synthesis procedure rather than a reflection of the seemingly basic nature of these compounds.

Electrochemical Impedance Spectroscopy

The results of the electrochemical impedance testing, measured by corrosion rate, for each compound and boric acid are shown in Table 3.

Table 3: Corrosion rate data of Boron Hydride Compounds

Compound	I_{corr} at 22 °C (µA)	I_{corr} at 80 °C (µA)
$Li_2B_{10}H_{10}$	8.887	20.311
$Na_2B_{10}H_{10}$	4.707	23.692
$K_2B_{10}H_{10}$	7.005	21.047
$Li_2B_{12}H_{12}$	3.528	22.384
$Na_2B_{12}H_{12}$	5.423	23.590
$K_2B_{12}H_{12}$	3.209	20.418
Boric Acid	20.260	39.966

From the data in Table 3 it can be seen that at both temperatures investigated each compound possessed a lower Icorr value than boric acid. The Icorr represents the amount of corrosion current or the electrochemical reaction at the interface between the steel and the compounds solution, the lower the current the lower the corrosion rate. (*27*) The Tafel plots, shown in Figure 11 , demonstrate the rate at which electron transfer is occurring between the solution of each compound and the working electrode, which in this case is the stainless steel coupon. When the test starts an anodic current is passed through the compound solution and to the coupon, represented as the bottom curve. Once that current reaches zero then a cathodic current is applied, represented by the top curve. The Icorr value is the intersection of the tangent line of the two curves produced. When considering these compounds as neutron absorbers for use in the presence of steel a low Icorr value is desired. The Tafel plots of boric acid and $Li_2B_{10}H_{10}$ at 22 °C and 80 °C are shown in Figure 11. Tafel plots for all compounds are shown in Appendix C.

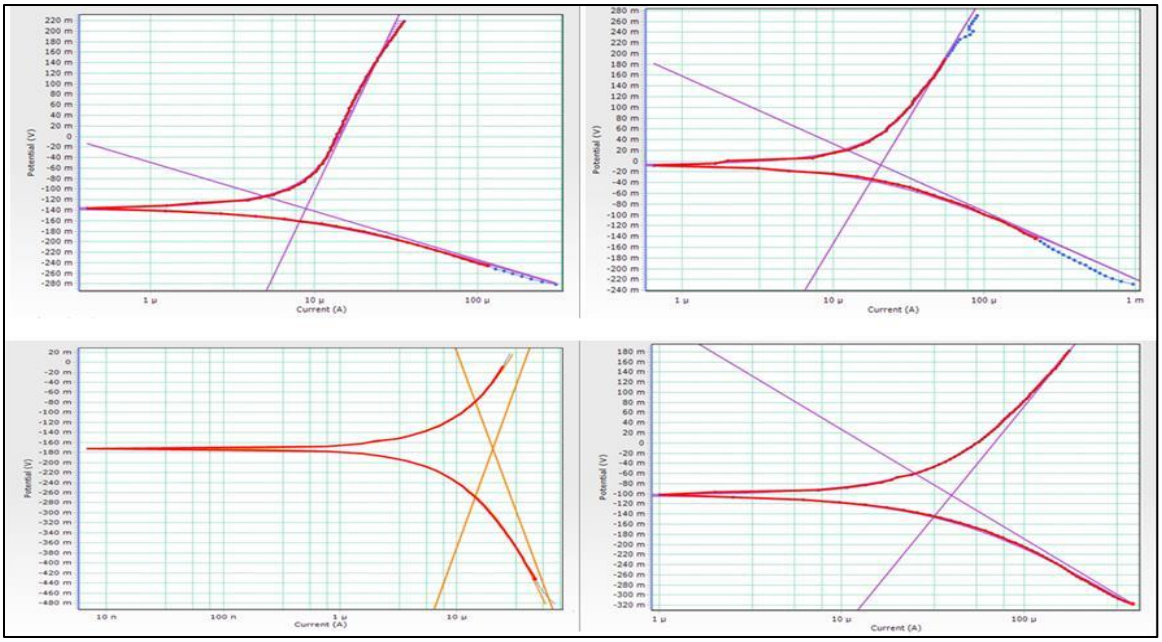

Figure 11: Tafel Plots for $Li_2B_{10}H_{10}$ (Top) and Boric Acid (Bottom) at 22 °C (left) and 80 °C (right)

It can be seen from these Tafel plots that the $Li_2B_{10}H_{10}$ at both temperatures has a higher y-axis value as the test switches from anodic current to cathodic current. This is evidence that in the presence of the $Li_2B_{10}H_{10}$ compound the steel is behaving more noble as compared to its behavior in the boric acid solution. Also, from the Tafel plots, the $Li_2B_{10}H_{10}$ solutions' cathodic current curve is observed to be asymetrical with the anodic current curve, unlike the boric acid with both curves being symetrical. This indicates passivation, meaning the $Li_2B_{10}H_{10}$ solution is loosing the ability to remove electrons from the metal. These results indicated that the $Li_2B_{10}H_{10}$ was less damaging to the steel coupon than boric acid. Similar results were found for each boron hydride compound.

CHAPTER IV

CONCLUSION

As the need for neutron absorption remains steady in the nuclear industry boron hydride compounds have been shown to be a viable alternative to boric acid, especially in emergency shut down situations. The synthesis of these compounds using cation exchange has been shown to be effective in producing the desired boron hydride salts while removing the initial triethyl ammonium cation. With a boron content of up to 80% by weight these compounds have almost five times as much boron as boric acid. This high boron content would decrease the total amount of material needed in an emergency. The solubility of these compounds has been shown to be over ten times higher than boric acid at room temperature and even higher at increased temperatures. This high solubility would further assist in an emergency situation by decreasing the overall volume of the water safety system. As the pH of these compounds is neutral and their corrosion of steel has been shown to be lower than boric acid at both 22 °C and 80 °C, the general safety concerns for these compound's interactions with containment vessels would be far less than boric acid. What is now needed is further testing of these compounds under irradiated conditions. Of interest is the stability of the boron cage, both the B_{10} and B_{12},

when radiation is encountered. If the boron cage of these compounds were to remain unbroken even after being irradiated the benefits of these compounds as neutron absorbers would be increased. As all of the components of each boron hydride compound are commonplace in the nuclear industry if the integrity of the cage were compromised it would be expected that no significant increase of adverse effects would be encountered. Further research is also necessary to determine the byproducts of these compounds after thermal neutron absorption.

REFERENCES

1. IAEA. World Statistics Nuclear Energy Around the World. http://www.nei.org/Knowledge-Center/Nuclear-Statistics/World-Statistics (accessed November 2014).

2. Mughabghab, S. F.; Divadeenam, M.; Holden, M. Neutron Cross Sections from Neutron Resonance Parameters and Thermal Cross Sections. http://ie.lbl.gov/ngdata/sig.htm (accessed November 2014).

3. IAEA. *Chemistry Programme for Water Cooled Nuclear Power Plants;* Marketing and Sales Unit, Publishing Section International Atomic Energy Association: Vienna, 2011.

4. Park, J. H.; Chopra, O. K.; Natesan, K.; Shack, W. J. *Boric Acid Corrosion of Light Water Reactor Pressure Vessel Materials;* U.S. Nuclear Regulatory Commission: Washington D.C., 2005.

5. IAEA. *IAEA Fukushima Daiichi Status Report -2 November 2011-;* International Atomic Energy Association: Vienna, 2011.

6. Bommaraju, T. V.; Adams, R. G. Corrosion Supression of Stainless Steel in Caustic Media. US5,154,860, October 13, 1992.

7. Suwattananont, N.; Petrova, R. S.; Zunio III, J. L.; Schmidt, D. P. Surface Treatment with Boron for Corrosion Protection. *2005 Tri-Service Corrosion Conference*, Newark, New Jersey, 2005; pp 5-27.

8. Stock, A. *Hydrides of boron and silicon,* 2nd ed.; Cornell University Press: Ithaca, New York, 1933.

9. Bregadze, I. B. S. V. I.; Sjoberg, S. Chemistry of Closo-Dodecaborate Anion $(B_{12}H_{12})^{2-}$: A Review. *Collection of the Czech Chemistry Community* **2002,** *67*, 679-695.

10. Lipscomb, W. N. *Boron Hydrides,* 4th ed.; W.A. Benjamin Inc.: New York, 1963.

11. Williams, R. E.; Ditter, J. Carboranes and Boranes; Polyhedra and Polyhedral Fragments. *J. Am. Chem. Soc.* **1973,** *10*, 7514-7516.

12. Muetterties, E. L.; Balthis, J. H.; Chia, Y. T.; Knoth, W. H.; Miller, H. C. Chemistry of Boranes, Salts and Acids of $B_{10}H_{10}^{2-}$ and $B_{12}H_{12}^{2-}$. *Inorganic Chemistry* **1963,** *3*, 23.

13. Kaczmarczyk, A.; Nichols, W.; Stockmayer, W. H.; Eames, T. B. Thermodynamic Properties of $B_{10}H_{10}^{2-}$ (aq) and $B_{12}H_{12}^{2-}$ (aq). *Inorganic Chemistry* **1968,** *7*, 50-62.

14. Nies, N. P.; Hulbert, R. W. Solubility Isotherms in the System Sodium Oxide -Boric Oxide-Water. *Journal of Chemical and Engineering Data* **1697,** *12*, 301-312.

15. Abi-Ghaida, F.; Laila, Z.; Ibrahim, G.; Naoufal, D.; Mehdi, A. New Triethoxysilylated 10-Vertex Closo Decaborate Clusters. Synthesis and Controlled Immobilization into Mesoprous Silica. *Dalton Transcrips* **2014,** *43*, 24-31.

16. Ittel, S. D.; Reynolds, G. A.; Zheng, M. Process for Improving the Oxidation Resistance of Carbon Nanotubes. US20100219738 A1, September 2, 2010.

17. Locher, G. L. Biological Effects and Therapeutic Possibilities of Neutrons. *American Journal of Roentgenology* **1936,** *36*, 1-13.

18. Kruger, P. G. Some Biological effects of Nuclear Disintegration products on Neoplastic tissue. *Pathology* **1940,** *26*, 181-191.

19. Farr, L. E.; Robertson, J. S.; Stickley, E. Physics and Physiology of Neutron-Capture Therapy. *Physiology* **1954,** *40*, 1087-1094.

20. Hosmane, N. S.; Fraken, A.; Zhang, G.; Srivastava, R. R.; Smith, R. Y. Synthesis and Crystal Structure of a Novel Fused Polyhedral Borane Dianion, $[B_{22}H_{22}]^{2-}$ Potential Precursor for use in Boron Neutron Capture Therapy of Cancer. *Main Group Chemistry* **2011,** *21*, 319-324.

21. Avdeeva, V. V.; Polyahova, I. N.; Goeva, L. V.; Malinina, E. A.; Kuznetsov, N. T. [2,6(9)-$B_{10}H_8(O)CCH_3]^-$ and [2,7(8)-$B_{10}H_8(OC(O)CH_3)^2]^{2-}$ Deravatives in Sythesis of Position Isomers of the $[B_{10}H_8(OC(O)CH_3)(OH)]^{2-}$ Anion with the 2,6(9)- and 2,7(8)- Arrangement of Functional Groups. *Russian Journal of Inorganic Chemistry* **2014,** *59* (11), 657-663.

22. OECD. *OECD Guideline For The Testing of Chemicals -Water Solubility-;* Organisation for Economic Co-operation and Development: Paris, 1995.

23. PAR. *Basics of Corrosion Measurements;* Priceton Applied Research: Oak Ridge, 2007.

24. Ocken, H.; Frattini, P.; Wood, C. J. Prospects for enriched boric acid in U.S. PWRs. In *Water Chemistry of Nuclear Reactor Systems*, 3rd ed.; Menzel, H., Ed.; British Nuclear Energy Society: Stevenage, 2000; Vol. II, pp 48-67.

25. NRC. *10 CFR Part 50 RIN 3150-AF06 Technical Specification;* Nuclear Regulatory Commision: Washington D.C., 1995.

26. Kinnard, M. *NRC Stepping up Monitoring at Oconee Plant;* Associated Press: Columbia, S.C., 2014.

27. Jones, D. A. *Principles and Prevention of Corrosion*, 2nd ed.; Prentice-Hall: Upper Saddle River, NJ, 1996.

APPENDIX

APPENDIX A

Solubility Data

Compound	% B	Temp (°C)	Grams used	Grams of B using % B	mls used	grams B/100 ml
Boric Acid (B(OH)3)	17.49	4	3.0143	0.5272	93.1	0.6
		22	3.0627	0.5357	63.8	0.8
		40	3.0091	0.5263	40.0	1.3
		60	3.0438	0.5324	26.2	2.0
$Li_2B_{10}H_{10}•2.6H_2O$	60.47	4	3.1150	1.8836	10.0	18.8
		22	3.0469	1.8425	5.7	32.3
		40	3.0523	1.8457	3.4	54.3
		60	3.0240	1.8286	2.1	87.1
$Na_2B_{10}H_{10}•0.7H_2O$	61.19	4	3.0174	1.8463	13.3	13.9
		22	3.0665	1.8764	8.9	21.1
		40	3.0431	1.8621	5.0	37.2
		60	3.0610	1.8730	3.2	58.5
$K_2B_{10}H_{10}•0.6H_2O$	52.20	4	3.0541	1.5942	24.8	6.4
		22	3.0155	1.5741	18.7	8.4
		40	3.0731	1.6042	9.7	16.5
		60	3.0045	1.5683	6.0	26.1
$Li_2B_{12}H_{12}•3H_2O$	61.89	4	3.0713	1.9008	11.3	16.8
		22	3.0668	1.8980	6.8	27.9
		40	3.0221	1.8704	4.5	41.6
		60	3.0312	1.8760	2.8	67.0
$Na_2B_{12}H_{12}•1.5H_2O$	60.42	4	3.0445	1.8395	14.0	13.1
		22	3.0471	1.8411	8.6	21.4
		40	3.0749	1.8579	5.8	32.0
		60	3.0517	1.8438	3.9	47.3
$K_2B_{12}H_{12}•1.3H_2O$	53.31	4	3.0127	1.6061	24.3	6.6
		22	3.0254	1.6128	17.6	9.2
		40	3.0769	1.6403	8.2	20.0
		60	3.0818	1.6429	5.1	32.2

APPENDIX B

NMR Spectra

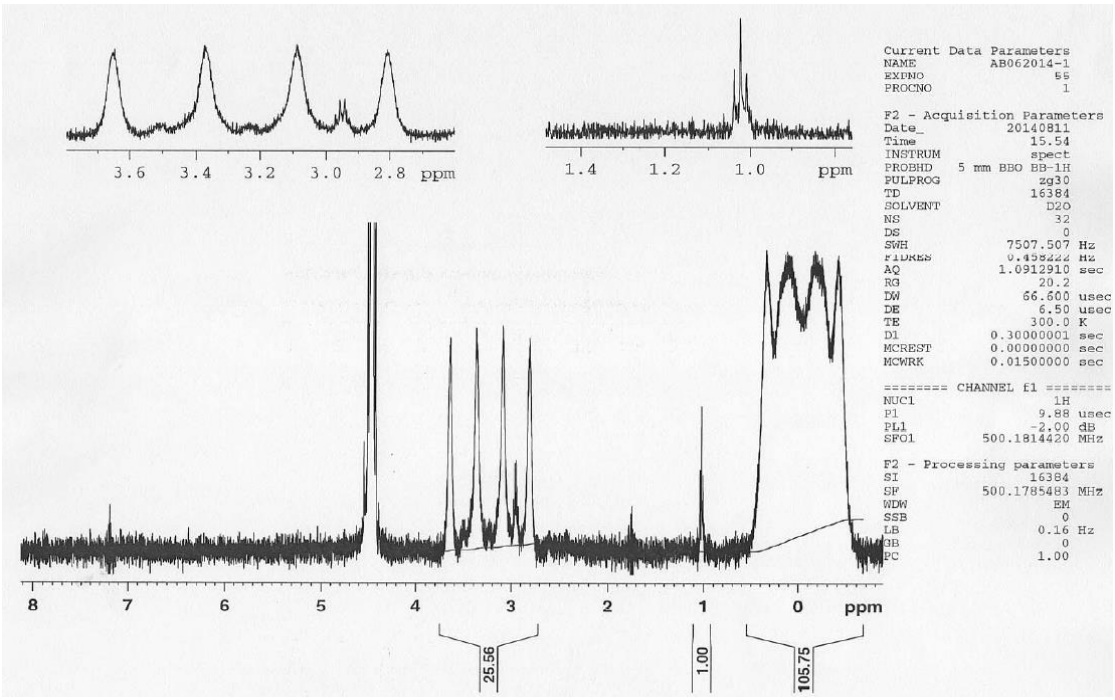

Figure 4: ^{1}H NMR of $Li_2B_{10}H_{10}$

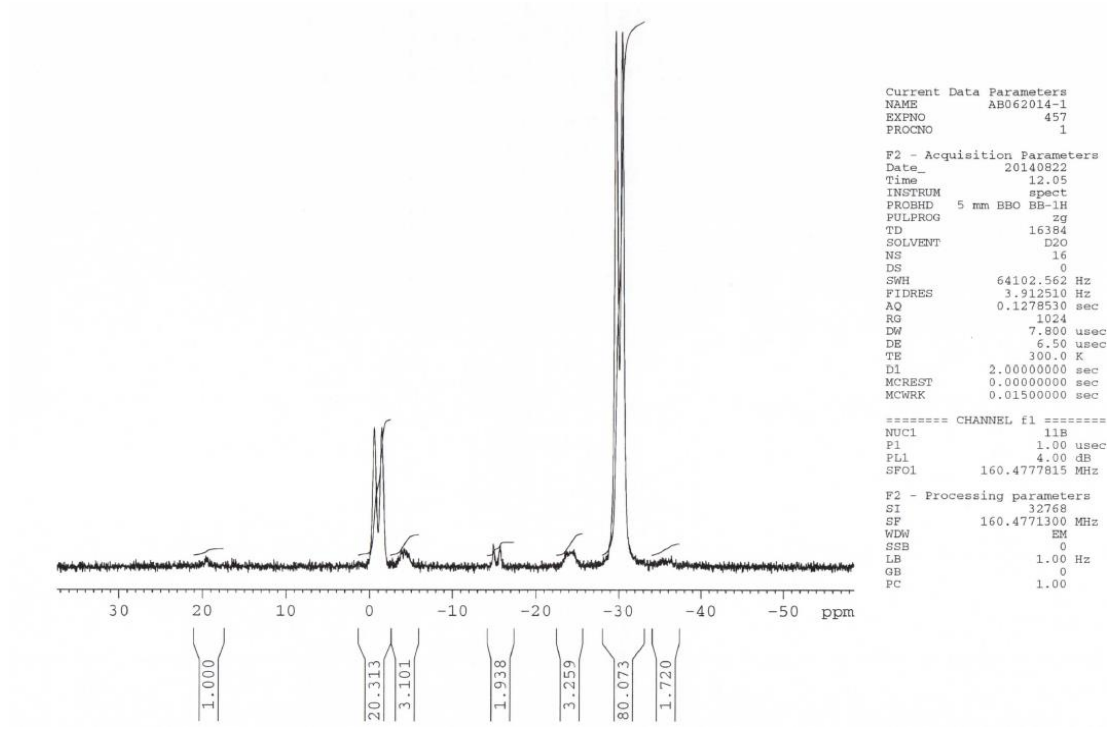

Figure 4-b : ^{11}B NMR of $Li_2B_{10}H_{10}$

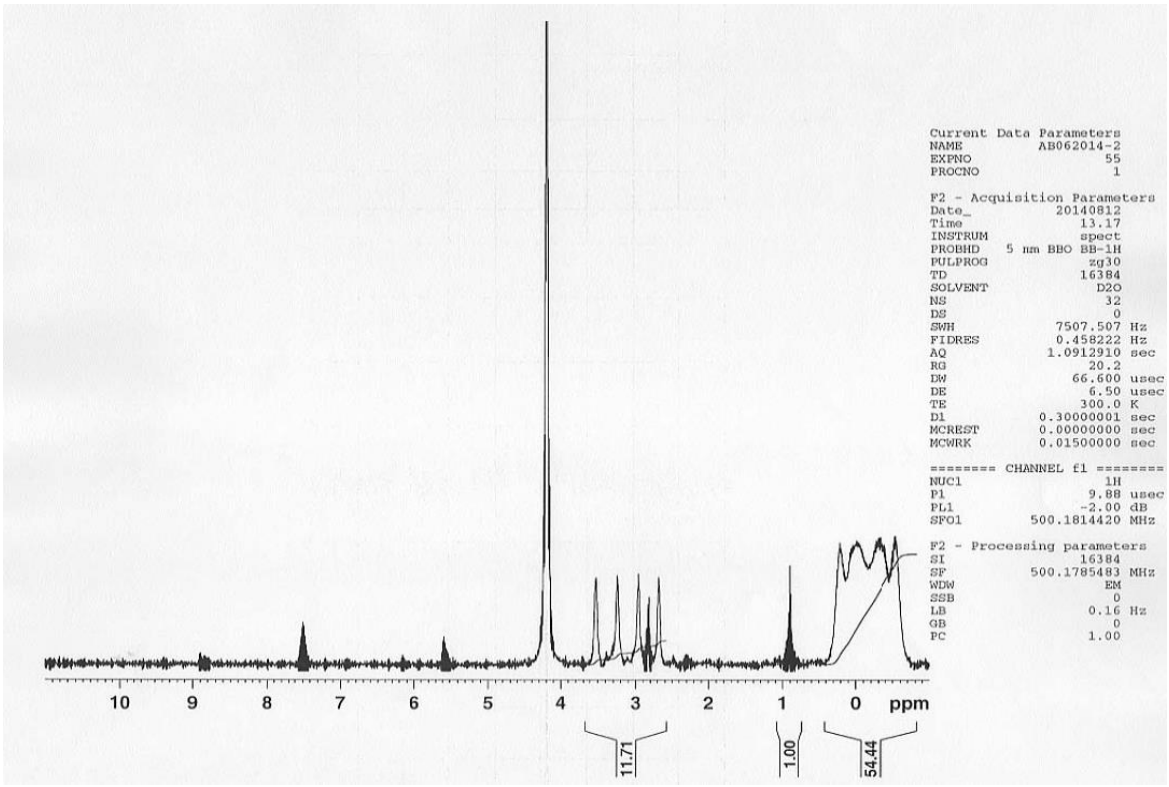

Figure 12: ^{1}H NMR of $Na_2B_{10}H_{10}$

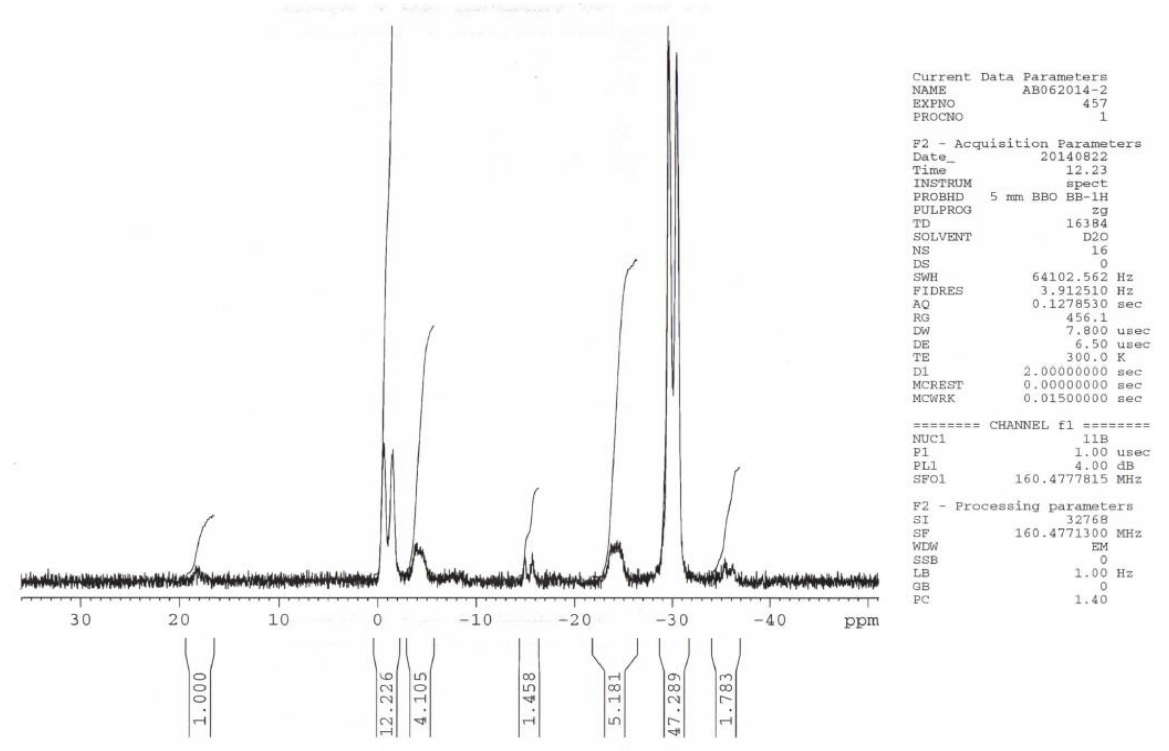

Figure 12-b: ^{11}B NMR of $Na_2B_{10}H_{10}$

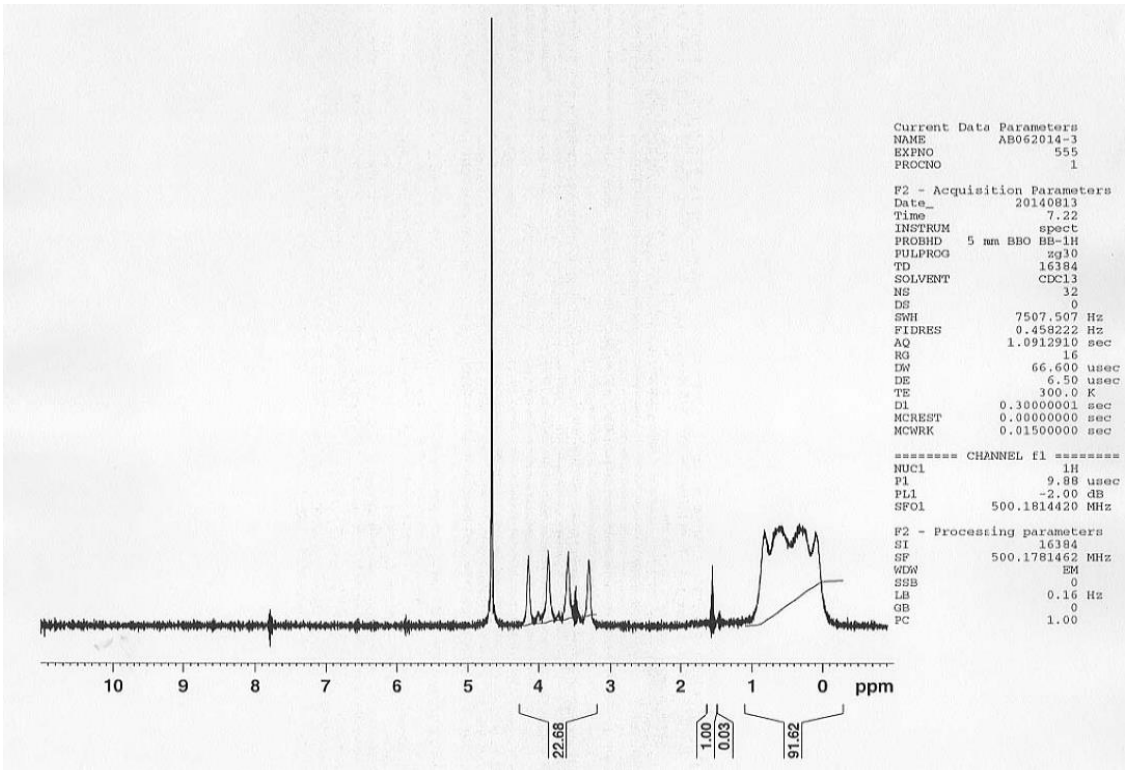

Figure 6-a: ^{1}H NMR of $K_2B_{10}H_{10}$

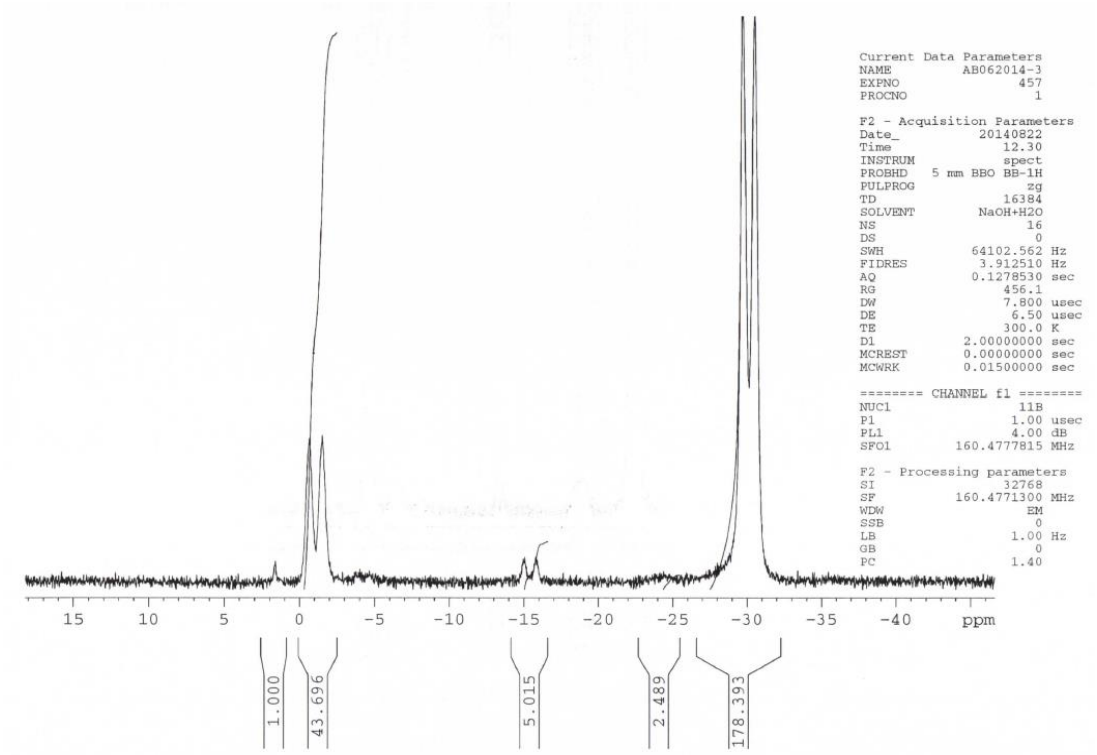

Figure 6: ^{11}B NMR of $K_2B_{10}H_{10}$

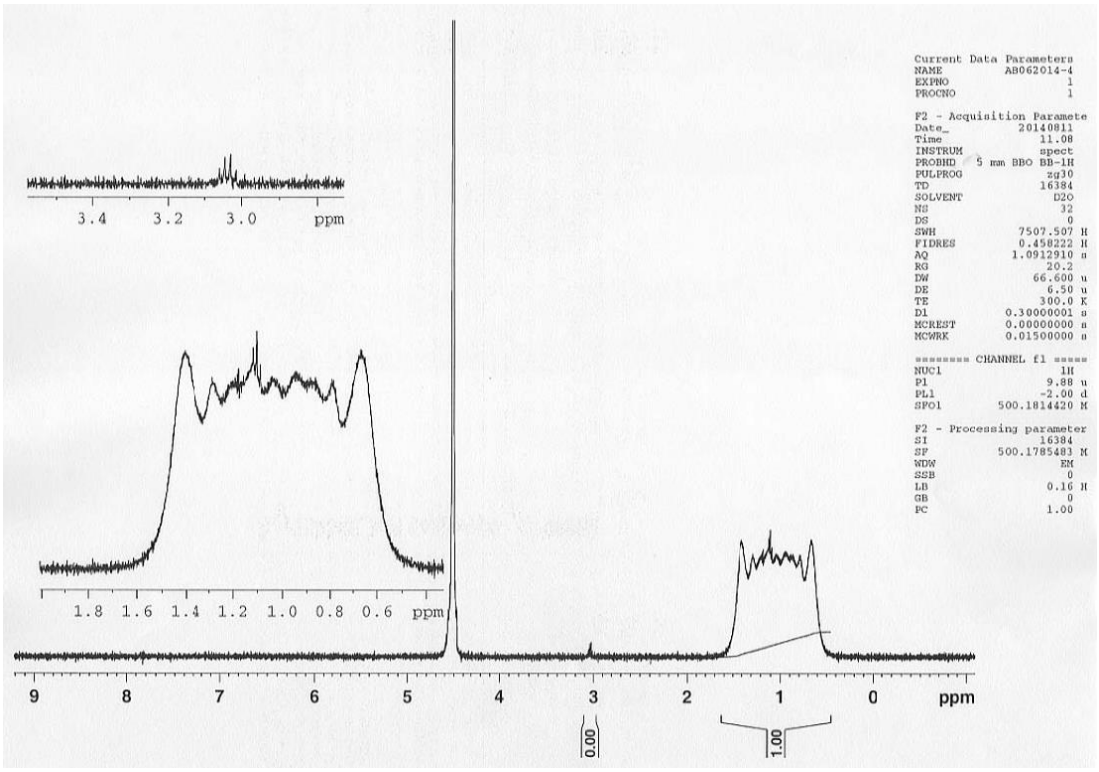

Figure 4: ^{1}H NMR of $Li_2B_{12}H_{12}$

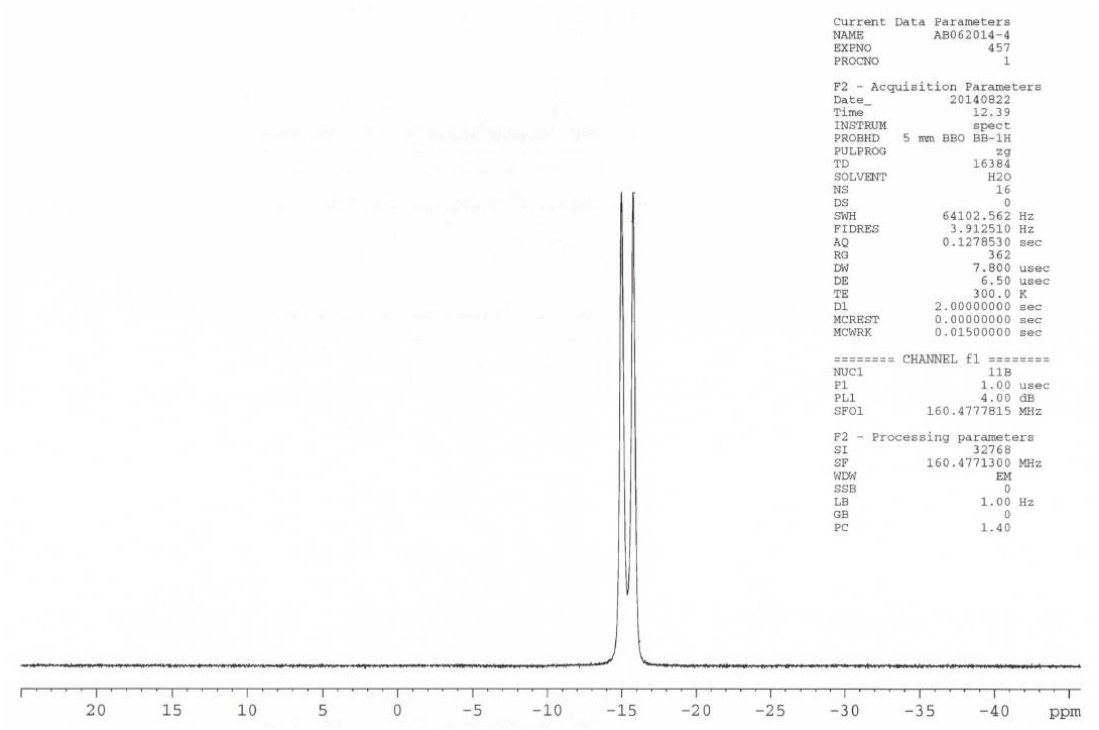

Figure 4-b: ^{11}B NMR of $Li_2B_{12}H_{12}$

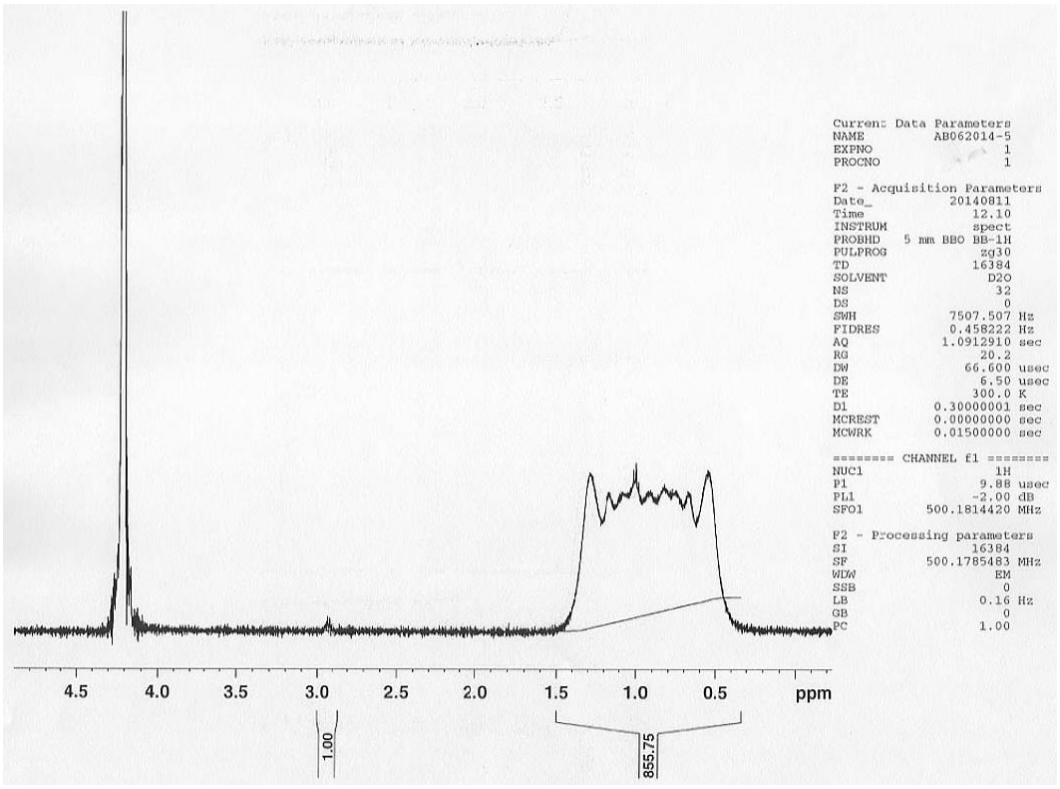

Figure 13: ^{1}H NMR of $Na_2B_{12}H_{12}$

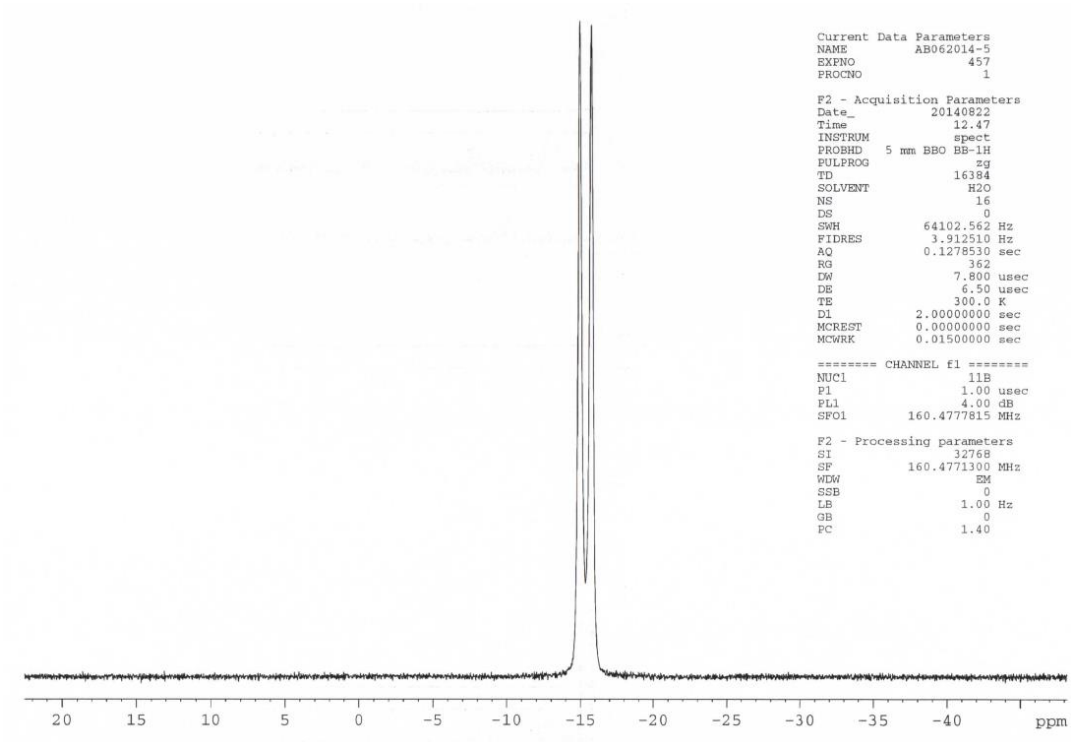

Figure 13-b: ^{11}B NMR of $Na_2B_{12}H_{12}$

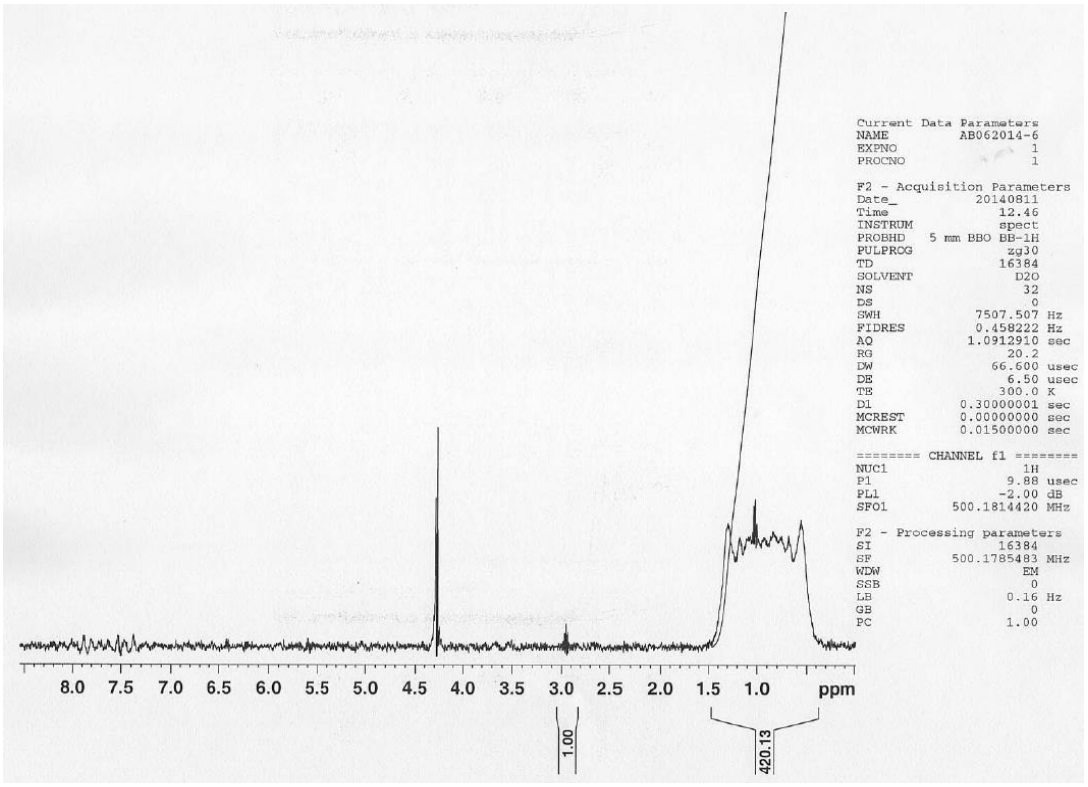

Figure 7-a: ^{1}H NMR of $K_2B_{12}H_{12}$

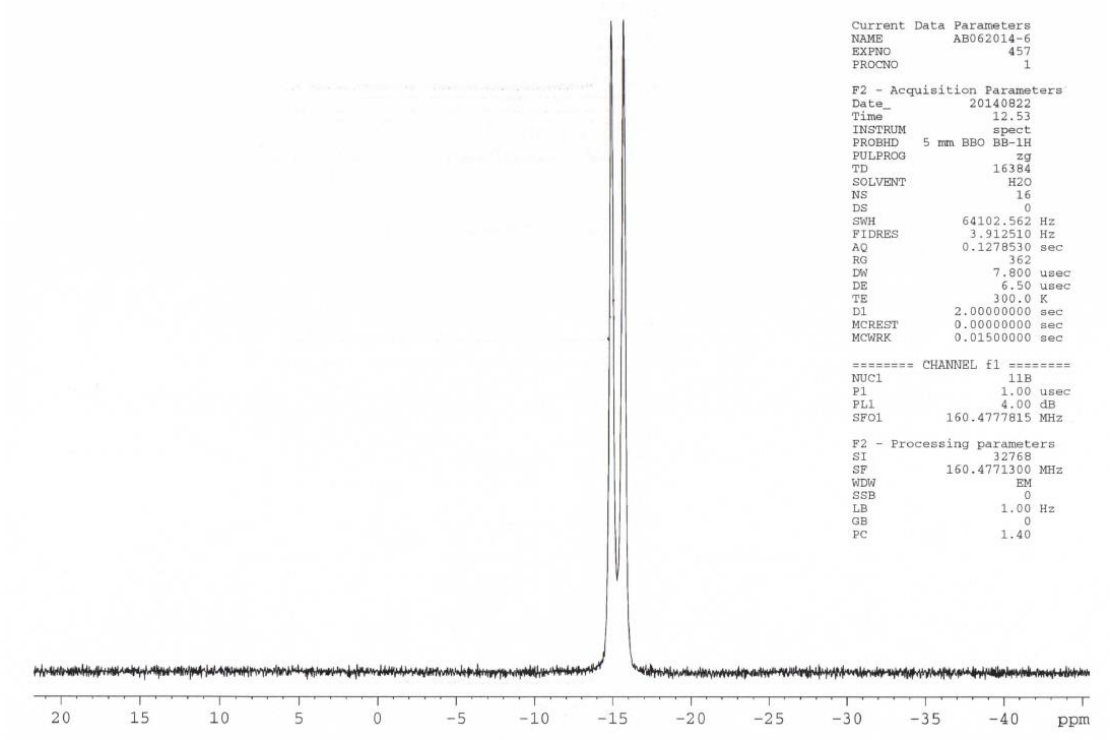

Figure 7: ^{11}B NMR of $K_2B_{12}H_{12}$

APPENDIX C

Tafel Plots of Boric Acid and Boron Hydride Compounds

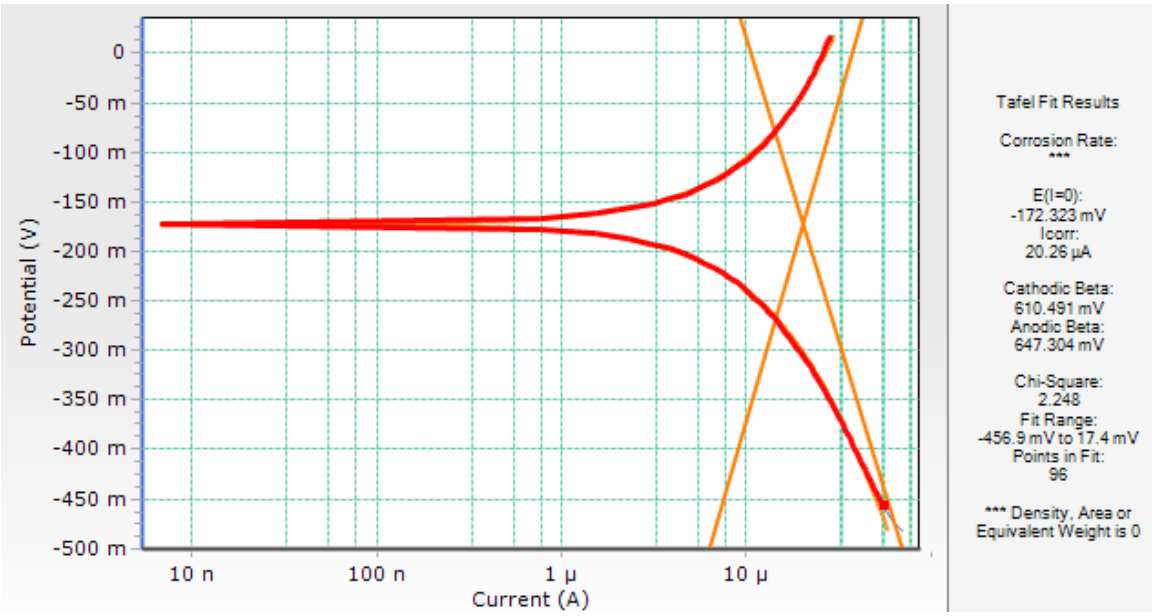

Figure 14: Tafel Plot of Boric Acid at 22 °C

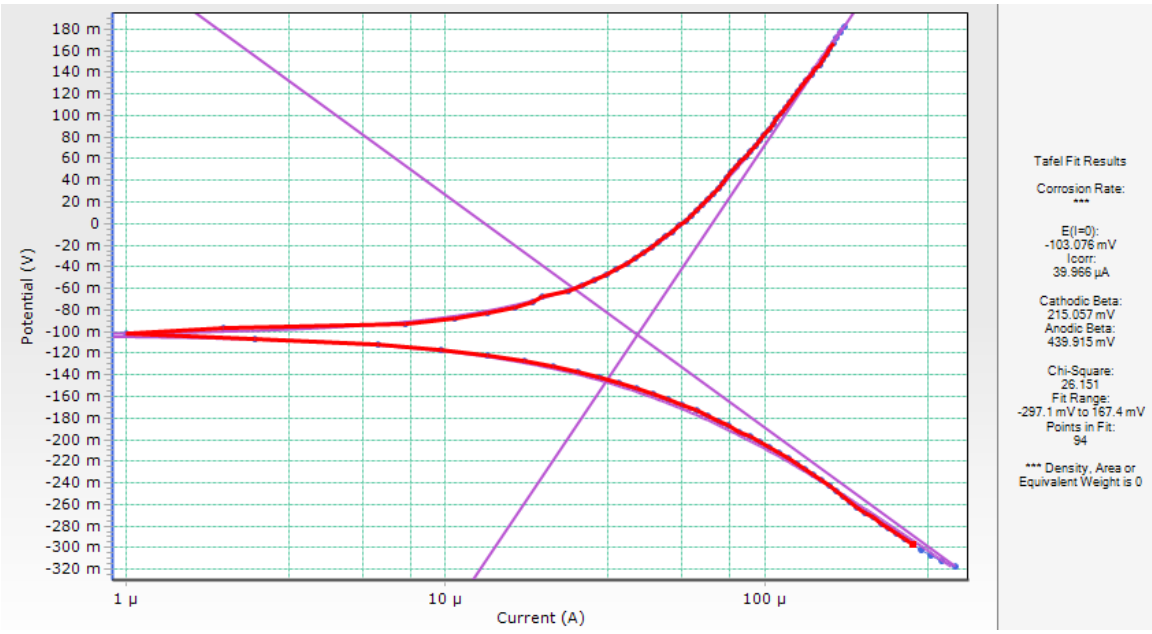

Figure 15: Tafel Plot of Boric Acid at 80 °C

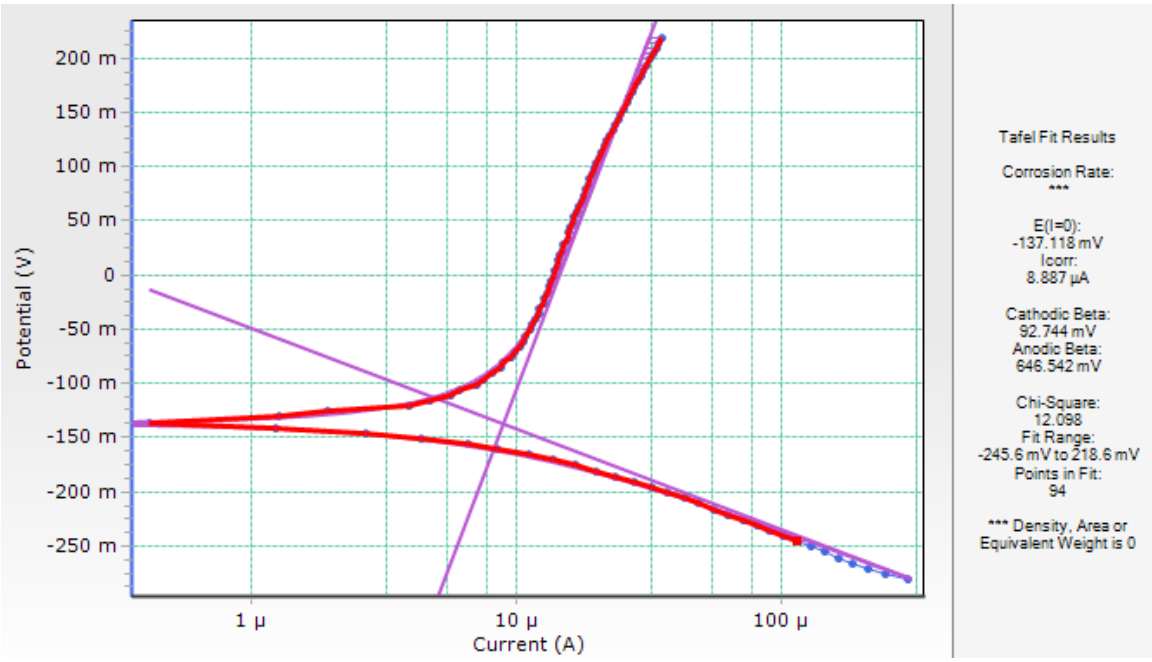

Figure 16: Tafel Plot of $Li_2B_{10}H_{10}$ at 22 °C

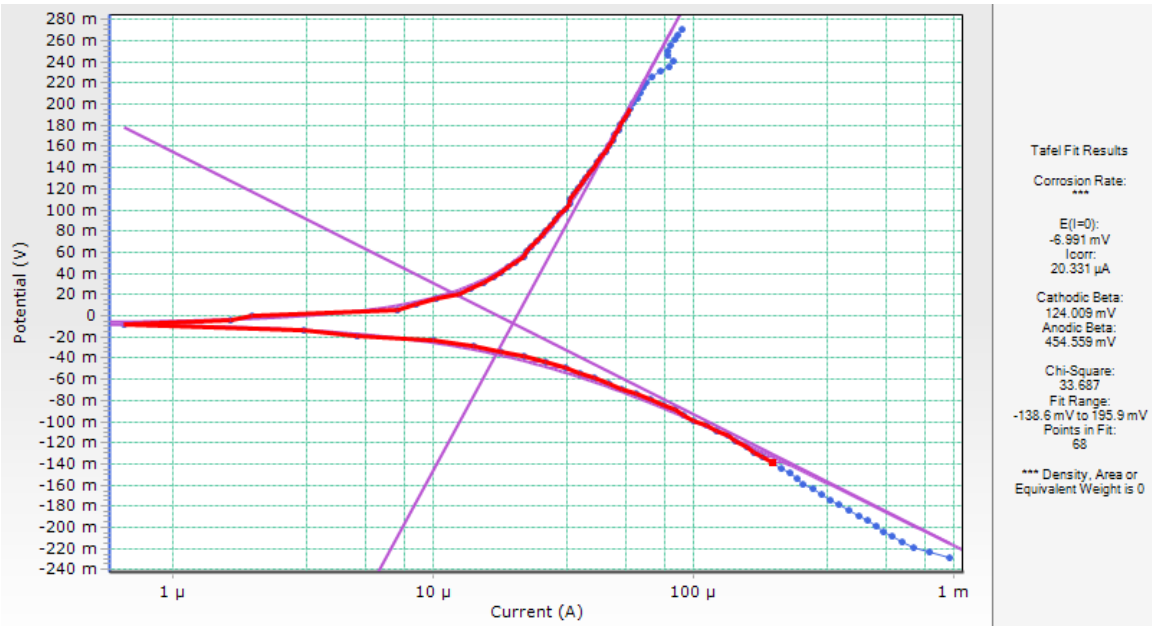

Figure 17: Tafel Plot of $Li_2B_{10}H_{10}$ at 80 °C

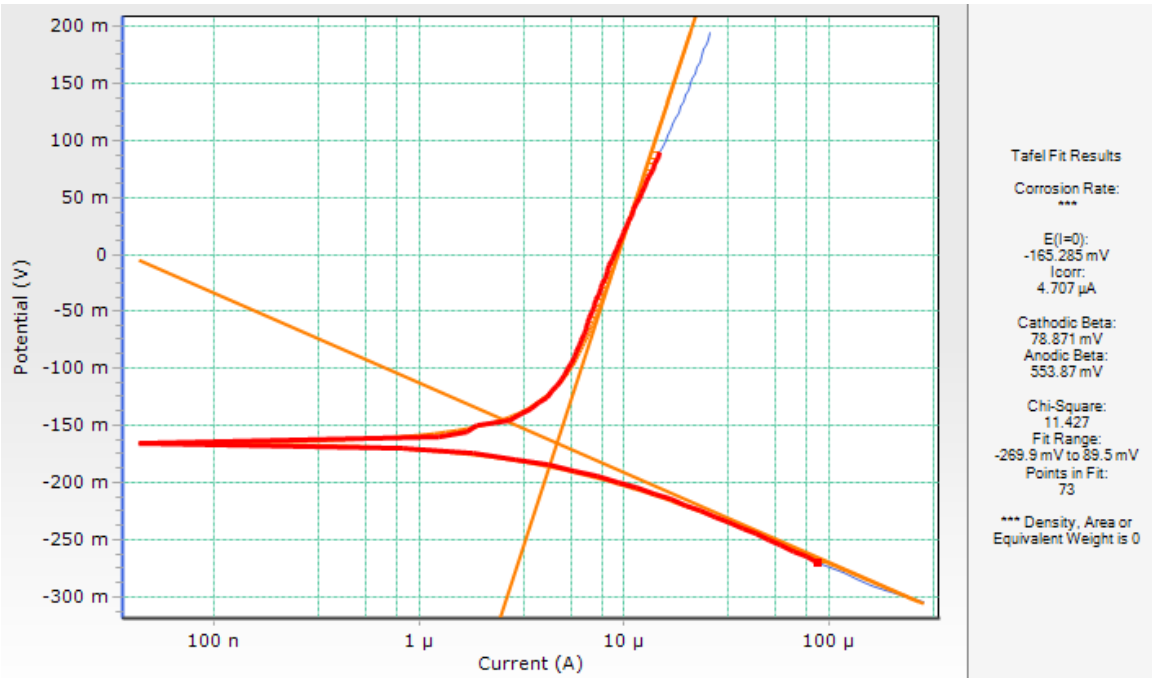

Figure 18: Tafel Plot of $Na_2B_{10}H_{10}$ at 22 °C

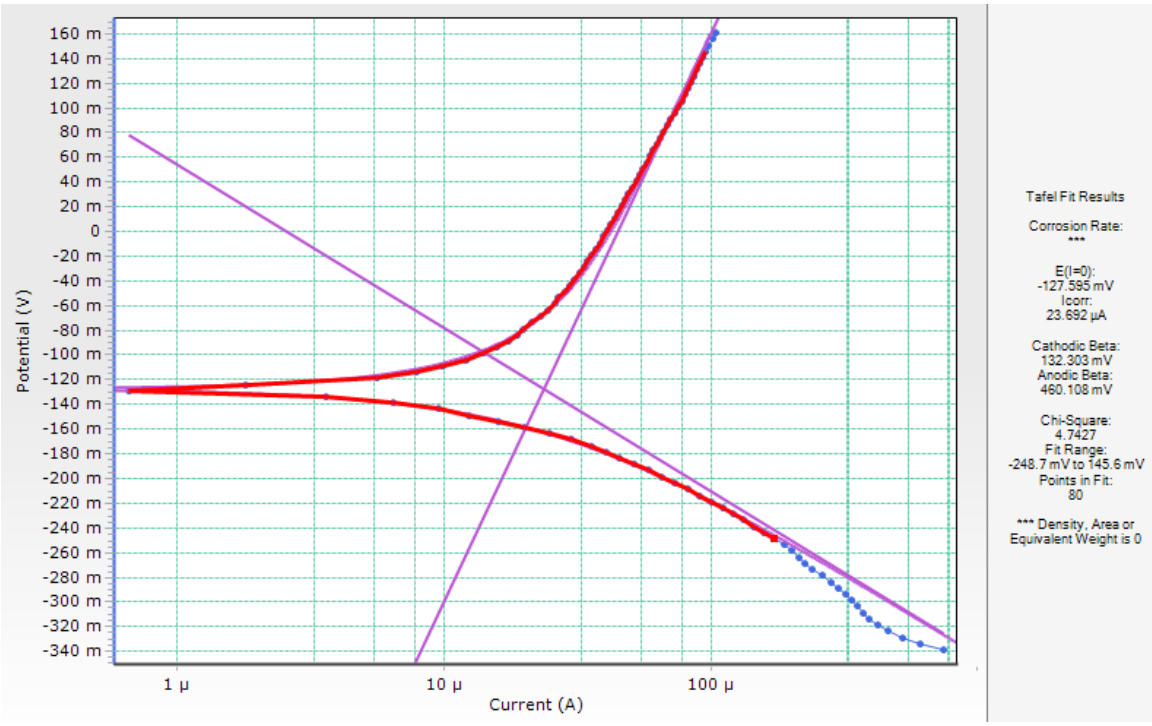

Figure 19: Tafel Plot of $Na_2B_{10}H_{10}$ at 80 °C

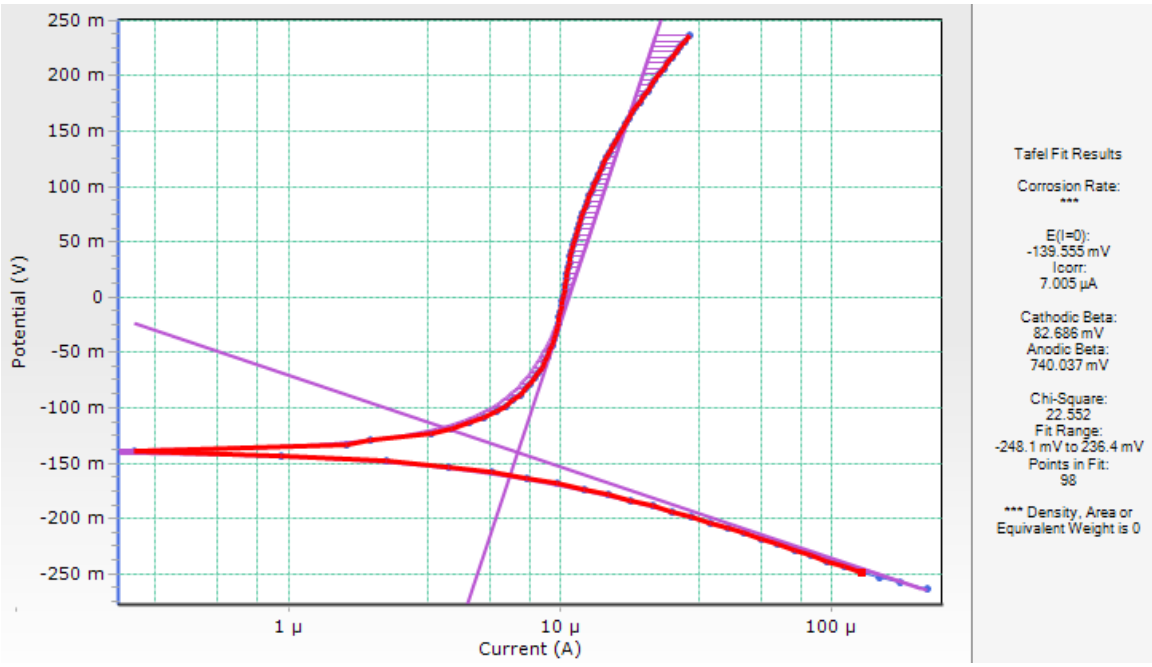

Figure 20: Tafel Plot of $K_2B_{10}H_{10}$ at 22 °C

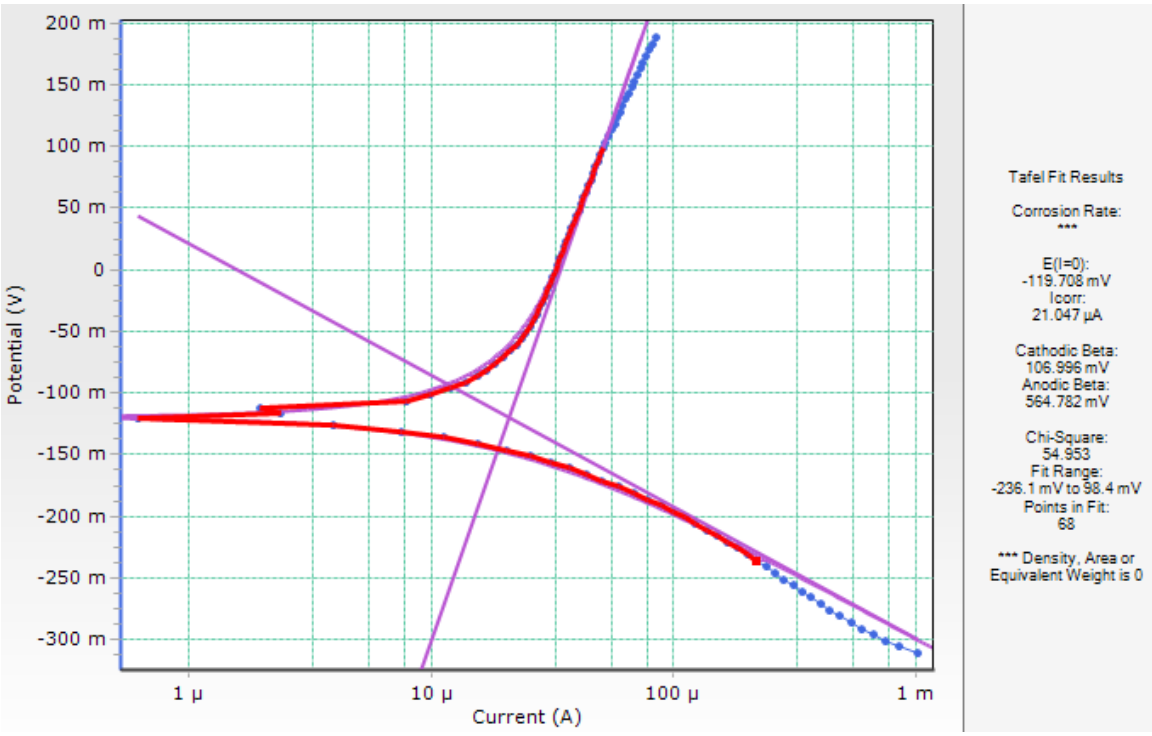

Figure 21: Tafel Plot of $K_2B_{10}H_{10}$ at 80 °C

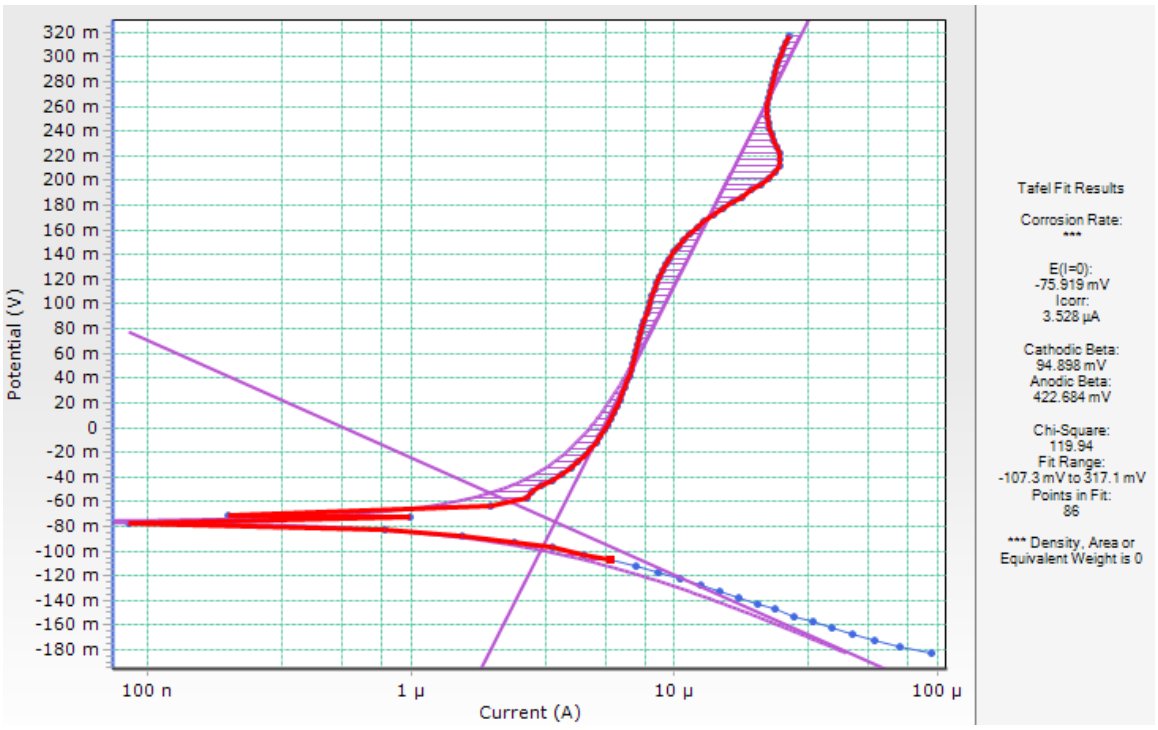

Figure 22: Tafel Plot of $Li_2B_{12}H_{12}$ at 22 °C

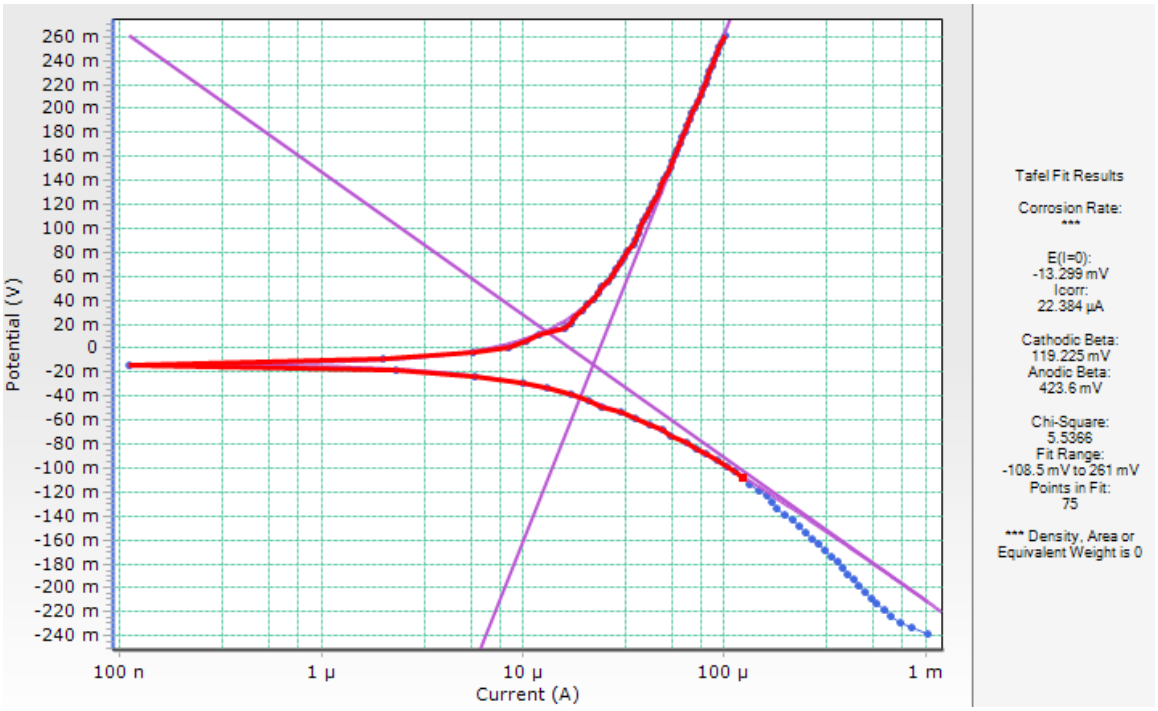

Figure 23: Tafel Plot of $Li_2B_{12}H_{12}$ at 80 °C

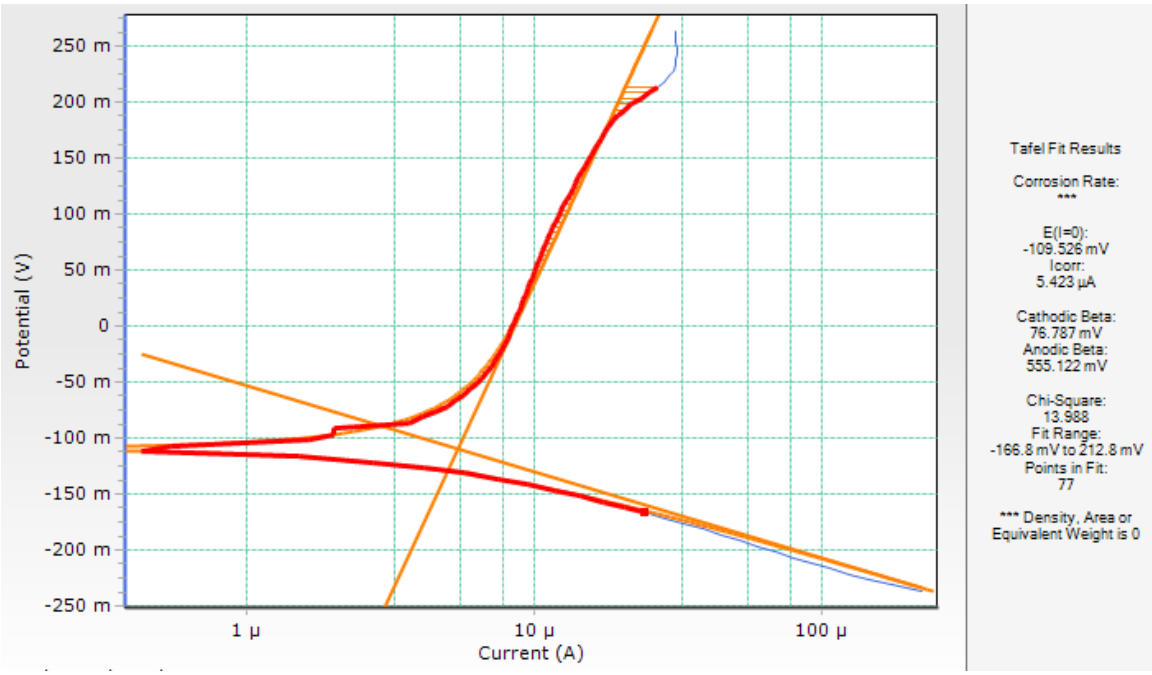

Figure 24: Tafel Plot of $Na_2B_{12}H_{12}$ at 22 °C

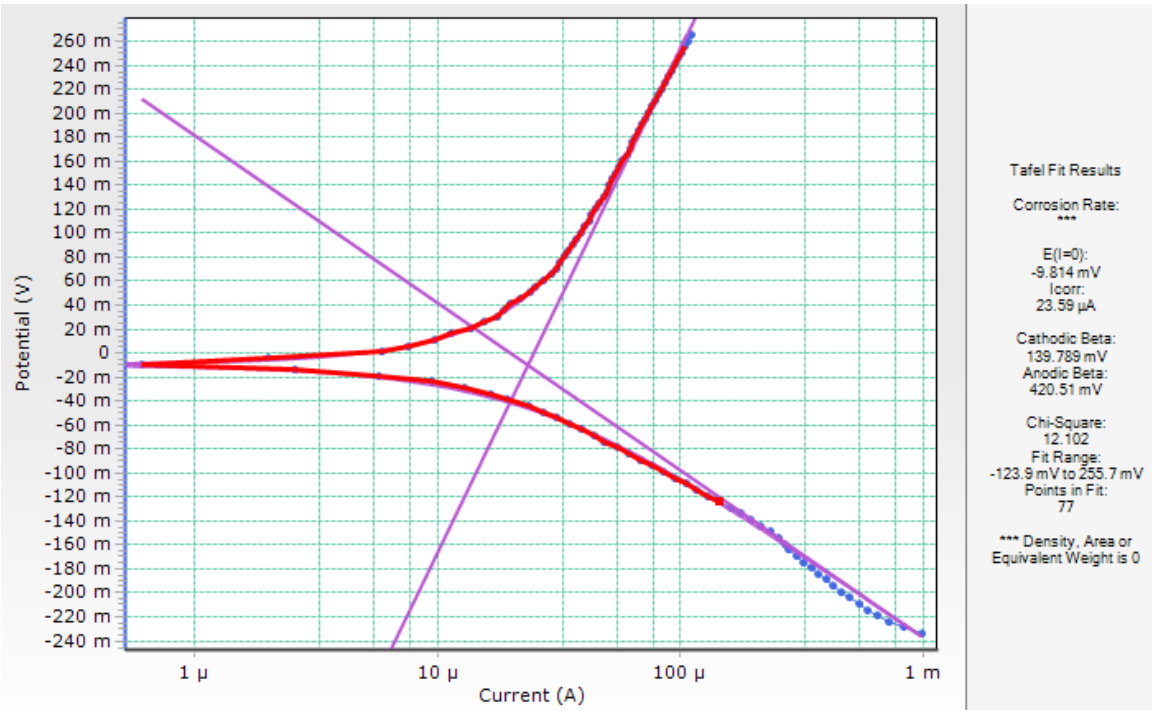

Figure 25: Tafel Plot of $Na_2B_{12}H_{12}$ at 80 °C

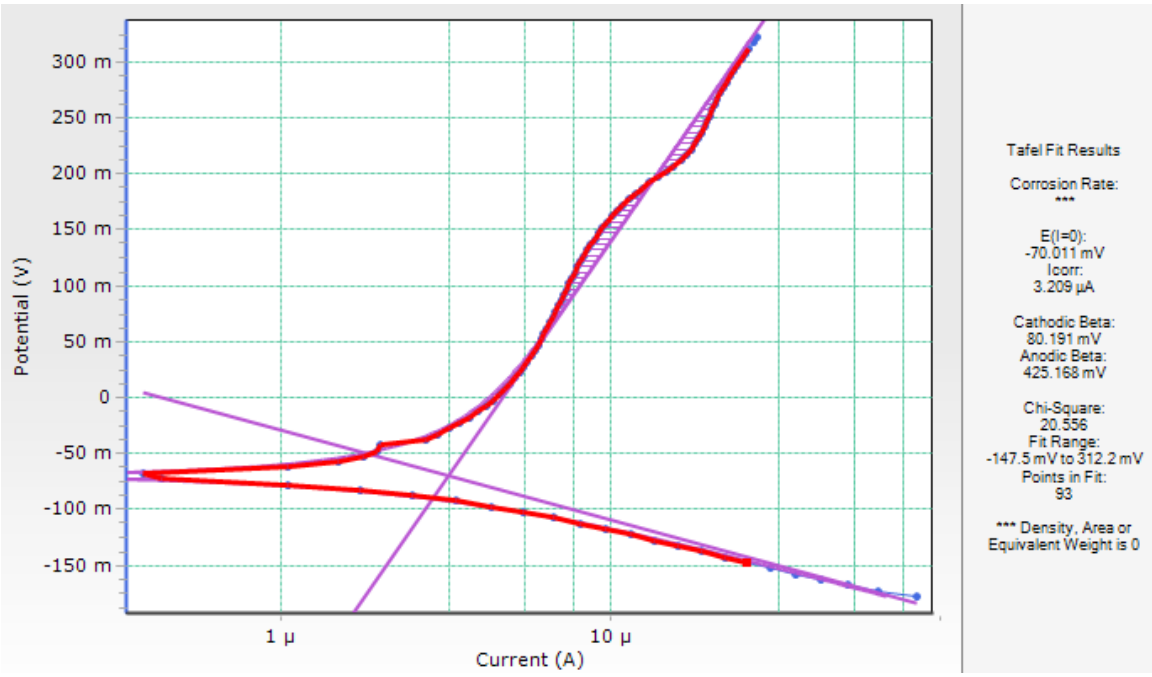

Figure 26: Tafel Plot of $K_2B_{12}H_{12}$ at 22 °C

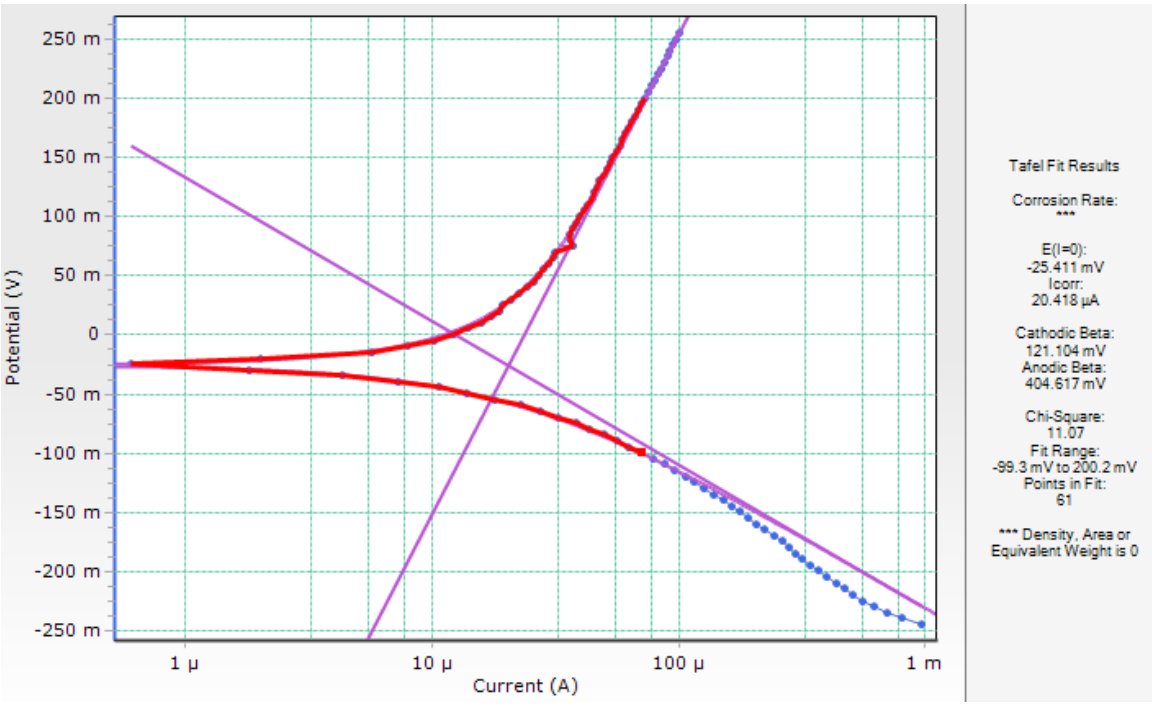

Figure 26: Tafel Plot of $K_2B_{12}H_{12}$ at 80 °C